
Masters Theses

Student Theses and Dissertations

Summer 1986

Experimental investigation of the effect of geological discontinuity conditions of rock splitting by blasting

Shijie Qu

Follow this and additional works at: https://scholarsmine.mst.edu/masters_theses



Part of the [Mining Engineering Commons](#)

Department:

Recommended Citation

Qu, Shijie, "Experimental investigation of the effect of geological discontinuity conditions of rock splitting by blasting" (1986). *Masters Theses*. 415.

https://scholarsmine.mst.edu/masters_theses/415

This thesis is brought to you by Scholars' Mine, a service of the Missouri S&T Library and Learning Resources. This work is protected by U. S. Copyright Law. Unauthorized use including reproduction for redistribution requires the permission of the copyright holder. For more information, please contact scholarsmine@mst.edu.

EXPERIMENTAL INVESTIGATION
OF THE EFFECT OF GEOLOGICAL DISCONTINUITY CONDITIONS
ON ROCK SPLITTING BY BLASTING

BY

SHIJIE QU, 1956-

A THESIS

Presented to the Faculty of the Graduate School of the

UNIVERSITY OF MISSOURI-ROLLA

In Partial Fulfillment of the Requirements for the Degree

MASTER OF SCIENCE IN MINING ENGINEERING

1986

Approved by

T5396
Copy 1
129 Pages

(Advisor)

Charles J. Hass

Peter G. Hansen

ABSTRACT

A series of modal scale, two borehole splitting test blasts was geometrically designed both with concrete and with Plexiglas. The discontinuities were all symmetrically located midway between split holes and were oriented perpendicular to the desired split plane. Sand and clay filled discontinuities of $1/16$, $1/8$ and $1/4$ inch width, and closed discontinuities were used. Both discontinuity frequency and width generally reduced the maximum successful split-hole spacing. The regularity and integrity of the split profile became poorer as the discontinuities were closer to the boreholes and the discontinuity width became greater, due to the cratering effect which occurred from the borehole to the near discontinuity. The discontinuities with rough planes tended to direct the path of the split and affect the split profile.

High speed photoelastic Plexiglas model tests indicated that radial cracking around boreholes was initiated by the dynamic shock waves and then extended by the rapidly expanding explosion gases. Shock waves were delayed and attenuated across discontinuities. Long cracks were created preferentially towards but stopped at, the neighboring discontinuities. In order to avoid the cratering effect and ensure the regularity and integrity of the final rock face, split holes should be located a distance away from discontinuities located perpendicularly across the desired split plane.

ACKNOWLEDGEMENTS

The author is deeply indebted to Dr. Paul Worsey, his advisor, for his continuous assistance and guidance throughout this investigation and the valuable suggestions made during the course of this experimental work, as well as the criticism and final editing of the thesis. Many thanks are extended to Dr. Charles Haas, his advisory committee member, for his assistance in this investigation and review and criticism of this thesis; and to Dr. Peter Hansen, his advisory committee member, for his encouragement and support as well as the review and criticism of this thesis.

The author is also grateful to Mr. John Tyler, electronics engineer at the Rock Mechanics and Explosives Research Center of the University of Missouri-Rolla, for his generous aid with the high speed photographic instrumentation of this work; to Mr. Jim Blaine, for his assistance in preparing many of the test models; to Mr. Qingshou Chen, a visiting scholar from Beijing, China, for his personal interest shown and his volunteer physical help in preparing the concrete; and to the UMR students, Michael Schlumpberger, Douglas Barlett, and Stephen Fiscor, for their help in running many of the experiments.

And finally, sincere thanks to the government of the People's Republic of China for its financial support, without which all of this would have been impossible.

TABLE OF CONTENTS

	Page
ABSTRACT.....	ii
ACKNOWLEDGEMENTS.....	iii
LIST OF ILLUSTRATIONS.....	vii
LIST OF TABLES.....	xiii
I. INTRODUCTION.....	1
A. CONCEPT OF ROCK SPLITTING.....	1
B. THE PROBLEM.....	4
C. IMPORTANCE OF THE INVESTIGATION.....	5
D. APPROACH TO THE PROBLEM.....	6
II. LITERATURE REVIEW.....	7
A. PREVIOUS WORK.....	7
B. MECHANICS OF ROCK SPLITTING.....	11
III. DESIGN AND METHOD.....	18
A. EXPLOSIVE SELECTION.....	19
B. BLASTHOLE DIMENSIONS.....	20
1. Concrete Test Models.....	20
2. Plexiglas Test Models.....	22
C. LOADING PROCEDURE AND INITIATION.....	22
1. Concrete Model Tests.....	22
2. Plexiglas Model Tests.....	23
D. TEST MODEL DIMENSIONS.....	23
1. Concrete Test Models.....	23

2. Plexiglas Test Models.....	27
E. DISCONTINUITIES AND FILLING CONDITIONS.....	28
1. Joint Set Number and Orientation.....	28
2. Joint Extent and Width.....	29
3. Filling Materials.....	29
F. INSTRUMENTATION OF PLEXIGLAS MODEL TESTS.....	30
1. Properties of Plexiglas.....	30
2. Description of Polariscopes.....	31
3. High Speed Camera.....	36
IV. RESULTS AND DISCUSSION	39
A. CONCRETE MODEL TESTS.....	39
1. Maximum Successful Split-hole Spacing for a Continuous Concrete Medium.....	39
2. Effect of Discontinuity Frequency.....	42
a. Single-Closed-Joint Model Tests.....	42
b. Two-Closed-Joint Model Tests.....	44
3. Effect of Filling Materials.....	47
a. Sand Filling.....	48
1) Joint Filling Width $t = 1/16$ Inch.....	48
2) Joint Filling Width $t = 1/8$ Inch.....	48
3) Joint Filling Width $t = 1/4$ Inch.....	49
b. Clay Filling.....	51
1) Joint Filling Width $t = 1/16$ Inch.....	51
2) Joint Filling Width $t = 1/8$ Inch.....	52
3) Joint Filling Width $t = 1/4$ Inch.....	52

4. Effect of Discontinuity Filling Width.....	54
5. Effect of Discontinuity Plane Roughness....	57
B. PLEXIGLAS MODEL TESTS.....	58
1. Continuous Model Test.....	58
2. Sand Filling Model Tests.....	62
3. Closed Discontinuity Model Test.....	65
V. CONCLUSIONS.....	66
VI. RECOMMENDATIONS.....	69
BIBLIOGRAPHY.....	71
VITA.....	79
APPENDICES	
A. PROPERTIES OF CONCRETE AND PLEXIGLAS.....	80
B. PHYSICAL PROPERTIES OF FILLING MATERIALS.....	84
C. WAVE TRAPS.....	85
D. DATA AND PHOTOGRAPHS OF CONCRETE MODEL TESTS.....	93
E. DATA AND PHOTOGRAPHS OF PLEXIGLAS MODEL TESTS....	105

LIST OF ILLUSTRATIONS

Figure	Page
1: Principles of Pre-shearing.....	13
2: Pre-split Fracture in Rock with a Hole Spacing of 2.5 ft.....	13
3: Concrete Model Test Borehole Explosive Loading Structure.....	21
4: Plexiglas Model Test Borehole Explosive Loading Structure.....	21
5: Dimensions of Concrete Model with One Discontinuity.....	26
6: Dimensions of Concrete Model with Two Discontinuities.....	26
7: Arrangement of Components of the Circular Polariscopes.....	33
8: Arrangement of the Instruments for High Speed Photography of Plexiglas Model Tests.....	35
9: Blasting Chamber and "Cordin" Synchronization Instrument for the High Speed Camera.....	38
10: The Inverse Relationship between Maximum Successful Split-hole Spacing and Rock Tensile Strength.....	43
11: Maximum Successful Split-hole Spacing S_m vs. Closed Discontinuity Frequency n	46

Figure	Page
12: Maximum Successful Split-hole Spacing S_m vs. Sand Filling Width t	56
13: Shock Wave Propagation Velocity v and Radial Cracking Velocity u vs. Radial Distance r	61
 Appendix	
C-1: Mechanics of Free Surface Spalling.....	90
C-2: Multiple Spalling of Free Surfaces.....	91
C-3: Wave Trap Mechanics.....	92
D-1: Continuous Concrete Model Test: Test C-1, S=5 in., A Failure.....	94
D-2: Continuous Concrete Model Test: Test C-3, S= 4 1/2 in., A Success.....	94
D-3: Single Closed Joint Concrete Model Test: Test C-6, S=4 1/2 in., A Success.....	95
D-4: Single Closed Joint Concrete Model Test: Test C-7, S=5 1/4 in., A Failure.....	95
D-5: Two Closed Joint Concrete Model Test: Test C-13, S=4 in., A Failure.....	96
D-6: Two Closed Joint Concrete Model Test: Test C-12, S=3 7/8 in., A Success.....	96
D-7: 1/16 in. Sand Filled, Two-Joint Concrete Model test: Test C-15, S=4 in., A Failure.....	97
D-8: 1/16 in. Sand Filled, Two-Joint Concrete Model test: Test C-16, S=3 7/8 in., A Success...	97

Appendix

Figure	Page
D-9: 1/8 in. Sand Filled, Two-Joint Concrete Model Test: Test C-21, S=3 7/8 in., A Failure..	98
D-10: 1/8 in. Sand Filled, Two-Joint Concrete Model Test: Test C-19, S=3 3/4 in.....	98
D-11: 1/4 in. Sand Filled, Two-Joint Concrete Model Test: Test C-22, S=4 1/4 in., A Failure..	99
D-12: 1/4 in. Sand Filled, Two-Joint Concrete Model Test: Test C-24, S=3 5/8 in., A Success..	99
D-13: 1/16 in. Clay Filled, Two-Joint Concrete Model Test: Test C-29, S=4 in., A Failure.....	100
D-14: 1/16 in. Clay Filled, Two-Joint Concrete Model Test: Test C-31, S=3 7/8 in., A Success..	100
D-15: 1/8 in. Clay Filled, Two-Joint Concrete Model Test: Test C-35, S=3 3/4 in., A Success..	101
D-16: 1/8 in. Clay Filled, Two-Joint Concrete Model Test: Test C-36, S=3 7/8 in., A Failure..	101
D-17: 1/4 in. Clay Filled, Two-Joint Concrete Model Test: Test C-39, S=4 in., A Failure.....	102
D-18: 1/4 in. Clay Filled, Two-Joint Concrete Model Test: Test C-41, S=3 5/8 in., A Success..	102
D-19: Grooved Discontinuity Concrete Model Test: Test C-43, S=4 7/8 in., A Failure. Split Extended to the Grooves' Bottom.....	103

Appendix

Figure	Page
D-20: Grooved Discontinuity Concrete Model Test: Test C-44, S=4 3/4 in., A Success. Split Extended to the Grooves' Bottom.....	103
D-21: Two-Closed-Joint Concrete Model Test: Test C-9, S=3 3/4 inch. Split within the Middle Section Deviated from Centerline.....	104
D-22: 1/8 in. Sand-Filled, Two-Joint Concrete Model Test: Test C-19, S=3 3/4 inch, Cratering Occurred from Boreholes to Discontinuities.....	104
E-1: Plexiglas Test No. 1: Continuous Plexiglas Model Test. 5.0 Microseconds after Firing.....	106
E-2: Plexiglas Test No. 1: Continuous Plexiglas Model Test. 7.5 Microseconds after Firing.....	106
E-3: Plexiglas Test No. 1: Continuous Plexiglas Model Test. 10.0 Microseconds after Firing....	107
E-4: Plexiglas Test No. 1: Continuous Plexiglas Model Test. 12.5 Microseconds after Firing....	107
E-5: Plexiglas Test No. 1: Continuous Plexiglas Model Test. 15.0 Microseconds after Firing....	108
E-6: Plexiglas Test No. 1: Continuous Plexiglas Model Test. 17.5 Microseconds after Firing....	108
E-7: Plexiglas Test No. 1: Continuous Plexiglas Model Test. 20.0 Microseconds after Firing....	109

Appendix

Figure	Page
E-8: Plexiglas Test No. 1: Continuous Plexiglas Model Test. 22.5 Microseconds after Firing....	109
E-9: Plexiglas Test No. 1: Continuous Plexiglas Model Test. 25.0 Microseconds after Firing....	110
E-10: Plexiglas Test No. 1: Continuous Plexiglas Model Test. 27.5 Microseconds after Firing....	110
E-11: Plexiglas Test No. 1: Continuous Plexiglas Model Test. 30.0 Microseconds after Firing....	111
E-12: Plexiglas Test No. 1: Continuous Plexiglas Model Test. 32.5 Microseconds after Firing....	111
E-13: Plexiglas Test No. 2: 1/16 in. Sand Filled Two-Joint Model Test.....	112
E-14: Plexiglas Test No. 2: 1/16 in. Sand Filled Two-Joint Model Test, Photographed after Figure E-13.....	112
E-15: Plexiglas Test No. 3: 1/8 in. Sand Filled Two-Joint Model Test.....	113
E-16: Plexiglas Test No. 3: 1/8 in. Sand Filled Two-Joint Model Test, Photographed after Figure E-15.....	113

Appendix

Figure	Page
E-17: Plexiglas Test No. 4: 1/4 in. Sand Filled Two-Joint Model Test.....	114
E-18: Plexiglas Test No. 4: 1/4 in. Sand Filled Two-Joint Model Test, Photographed after Figure E-17.....	114
E-19: Plexiglas Test No. 5: Two Closed Joint Model Test.....	115
E-20: Plexiglas Test No. 5: Two Closed Joint Model Test, Photographed after Figure E-19.....	115
E-21: Post-test Picture of Test No. 1, Showing the Pattern of Cracks in the Continuous Plexiglas Test Model.....	116
E-22: Post-test Picture of Test No. 4, Showing the Cratering Effect in the 1/4 in. Sand Filled Two-Joint Plexiglas Test Model.....	116

LIST OF TABLES

Table	Page
I. DATA OF THE MAXIMUM SUCCESSFUL SPLITHOLE SPACING FOR THE CONTINUOUS CONCRETE.....	41
II. DATA OF CLOSED JOINT MODEL TESTS.....	45
III. DATA OF SAND-FILLED, TWO-JOINT CONCRETE MODEL TESTS.....	50
IV. DATA OF CLAY-FILLED, TWO-JOINT CONCRETE MODEL TESTS.....	53
V. MAXIMUM SUCCESSFUL SPLIT-HOLE SPACING S_m AND CLOSED-DISCONTINUITY FREQUENCY n	55
VI. MAXIMUM SUCCESSFUL SPLIT-HOLE SPACING S_m AND SILICEOUS SAND FILLING WIDTH t	55
VII. MAXIMUM SUCCESSFUL SPLIT-HOLE SPACING S_m AND CLAY FILLING WIDTH t	55
VIII. DATA FOR CONTINUOUS PLEXIGLAS MODEL TEST.....	60
 Appendix	
A-I. PROPERTIES OF THE FIRST MIX OF CONCRETE.....	81
A-II. PROPERTIES OF THE SECOND MIX OF CONCRETE.....	82
A-III. PROPERTIES OF PLEXIGLAS.....	83

I. INTRODUCTION

A. CONCEPT OF ROCK SPLITTING

In conventional blasting, explosives have usually been used in such a way so as to destroy the quality of, and induce cracks and fractures into, rock masses. The result is rough and uneven final rock faces, with fractures produced by the explosive penetrating back into the rock to a considerable extent. Working close to a poor rock face is unsafe. Scaling and support of the uneven and cracked final rock face is expensive. Using perimeter control blasting techniques, in which a continuous and clear final rock face can be produced by splitting the rock at the desired perimeter through the firing of a series of linear explosive charged boreholes, these kind of problems may be eliminated.

The term "rock splitting" is used for this experimental work as it possesses the general characteristics of the perimeter control blasting techniques. To understand rock splitting, as well as the problems associated with its applications which are studied through this work, it is necessary to give a general description of the available perimeter control techniques to date.

1. Line Drilling. Line drilling was the first of the developed perimeter control techniques. A line of parallel boreholes are drilled at very close spacings, normally 2 to 4 borehole diameters (Dupont, 1977), and are usually left

unloaded. Extremely light explosives have occasionally been used and fired as the last row of the main round.

In this technique, a plane of weakness is created to which the primary blast can break and, to some extent, reflects the stress waves produced by the blast, reducing the shattering and stressing in the finished final rock face. Therefore, a final rock face with a certain stability and integrity may be obtained. In the extremely light loading case, the explosive charges are used to initiate cracks along the line and are fired as the last row of the main round of the bulk blasts.

2. Smoothwalling. Smoothwalling is another perimeter control technique used when the rock face from bulk blasting is unstable and irregular in shape. It involves a row of holes at the perimeter of the excavation that is more lightly loaded with decoupled charges and more closely spaced and usually of smaller borehole diameter than other holes in the blast round. The smooth blastholes are fired after the main blast and the excavation of the rock pulled off from the main blast.

3. Buffer Blasting. Buffer blasting comprises light loading of the blast holes in the final row of a bulk drill pattern fired as the last row of the main round such that back break is reduced and the final rock face integrity is not so severely affected as that from fully loaded bulk blast holes. There are two ways of reducing charges. These are, by increasing the decoupling ratio thereby reducing the amount of the explosive or, by reducing the borehole diameter. In both

cases of light loading the drill pattern is generally contracted in for the last row for both burden and spacing to compensate for the reduction of loading.

4. Pre-split Blasting. Pre-split blasting is a technique used to provide smooth excavation profiles of reduced damage during blasting by pre-forming a continuous fracture between parallel boreholes lightly charged with decoupled explosives along the line of the required surface (Worsey, 1984). Pre-split holes are drilled at spacings usually ranging from 8 to 15 borehole diameters (Mellor, 1976; Worsey, 1985). A decoupling ratio of 2 to 5 is commonly used depending on the rock mass strength, economics versus desired results, and the explosive type. The annulus between the explosive charge and the borehole wall cushions the dynamic stress wave, therefore crushing and cracking of the rock around the pre-split holes are reduced. Fracture extension from the primary blast will be prohibited by the pre-formed split, and thus, the integrity of the final rock face can be protected.

5. Fracture Control Technique. In this technique, pre-split holes are notched along their length, in line with the panel. Light propellant or extremely light high explosive charges are used and are simultaneously initiated to provide a planar split in the rock along the panel, by propagation of the notches, without formation of radial cracks.

B. THE PROBLEM

It has been recognized, both from experience and experimental results, that geological discontinuities such as jointing systems, faults and mud seams present in rock masses have a considerable effect on the success of perimeter control blasting operations and the results of rock blasting in general (Drake, 1952; Ash, 1967; Johansson and Persson, 1970; Dupont, 1977; McKown, 1984). In order to understand the mechanics of rock splitting in perimeter blasting by explosives and improve the effectiveness of these rock blasting techniques, the effects of geological discontinuities need to be evaluated.

Although several research programs on perimeter control blasting, especially on pre-split blasting, have been undertaken up to the present time, this research has mainly been concerned with continuous materials and the effects of geological discontinuities have received only limited attention. In most cases of field practice, drill patterns as well as loading procedures are generally determined from full-scale test panels and personal experience, as the in-situ rock mass is, in the majority of common cases, a discontinuous medium with some kind of geological structure, and there are no hard and fast design rules which establish the relations between geological discontinuities and borehole patterns.

The purpose of this investigation is to examine the effects of geological discontinuities on the success of perimeter blasting (specifically pre-splitting) by undertaking a program of model blast tests in which major attention is focused on the discontinuity frequency, width, profile and filling conditions. The mechanics involved in the fracture process under these conditions are also analyzed.

C. IMPORTANCE OF THE INVESTIGATION

It is evident from the literature review that geological discontinuities, namely, joints, faults and mud seams etc. present in in-situ rock masses, have a considerable but relatively undetermined influence on the success of a perimeter blasting operation, specifically pre-splitting (hereafter termed rock splitting). Specifically, no pertinent investigations have been reported as to having either quantitatively or qualitatively examined the effect of geological discontinuity conditions on the maximum successful spacing of split boreholes. Although a complete evaluation of geological discontinuities under all conditions is beyond the scope of this investigation, a preliminary examination would be both realistic and valuable in order to identify the levels of magnitude in, and the importance of, the relationship between discontinuity width, frequency, discontinuity filling conditions, and the maximum successful spacing and the split profile from split blasting by high explosives. The results of the investigation may then serve as a basis of

justification for more extensive studies which would ultimately address the question as to a need for more accurate design specifications for split blasting in jointed and other discontinuous rock masses.

D. APPROACH TO THE PROBLEM

It would be impossible to simulate and examine all combinations of splitting in the presence of geological discontinuities under field conditions. Orientation of any discontinuity such as jointing, faults or mud seams is a spatial variable with respect to the required fracture plane. In addition, two or three sets of discontinuities may exist simultaneously. Filling conditions may vary from one site to another. Considering all the possible situations that may be met in the field, there would be an infinite number of combinations to be investigated which would need an infinite amount of time and work. Therefore, a more practical approach to the problem is to simulate geological discontinuities within concrete blocks which are geometrically designed to simulate parallel joint planes located midway between adjacent split holes and perpendicular to desired split planes. Simultaneous initiation of the boreholes was used to simulate field split blasting operations. Similarly, Plexiglas model test blasts were made, incorporating high speed photographic analysis, to examine the dynamic stress propagation process and the fracturing process during split blasting when geological discontinuities exist.

II. LITERATURE REVIEW

A. PREVIOUS WORK

Pre-splitting may be defined as a technique used to protect final excavation profiles from the disturbance from bulk blasts by pre-forming a continuous fracture plane between parallel boreholes lightly charged with decoupled explosives along the line of the required surface (Worsey et al., 1981, Ratan and Dhar, 1976).

Pre-splitting boreholes are drilled in a panel and are oriented parallel to one another at spacings normally varying between 8 to 15 borehole diameters (Langefors and Kihlstrom, 1963; Mellor, 1976; Worsey, 1985). The decoupling ratio, which is the ratio of borehole diameter to the borehole charge diameter, normally ranging from 2 to 5, is used specifically to damp the dynamic stresses and prevent overbreak at the immediate vicinity of the borehole (Landefors and Kihlstrom, 1963, Mellor, 1976, Ratan and Dhar, 1976).

The first application of the pre-splitting technique was made by D. K. Holmes at the Lewiston Power Plant. It was latter applied in the Niagara Power Project (Paine, Holmes and Clark, 1961). The excellent results of these applications of the pre-splitting technique offered new possibilities to reduce overbreak and ground vibrations and, allow protection of the competence of the final rock face. However, a variety of problems associated with its applications have not been

investigated in depth. A major area is the effect of geological discontinuities on the outcome of a rock splitting operation.

Field observations and measurements were made by Trudinger(1973) during the construction of the Kangaroo Creek Dam in South Australia where the pre-splitting technique was used for the forming of the final excavation profiles. The joints and mud seams present in the rock mass were found to have a considerable influence on the quality of pre-split batters and Trudinger concluded that the orientation of the predominant geological discontinuities was a critical important factor with respect to the result of a pre-split blasting operation. Trudinger also specifically reported that where the angles between the required batters and the foliation were less than 25 degrees, pre-split results would be unsatisfactory; between 25 and 40 degrees the pre-split planes followed paths partly along the foliation and partly across the fabric of the rock; and where greater than 40 degrees, the resulting presplit planes occurred almost entirely across the fabric.

Worsey (1981) verified the conclusions reached by Trudinger from his field observations during highway construction projects in Scotland and his analyses of a series of laboratory resin and concrete model tests.

When a single borehole in a continuous medium is explosively loaded many short cracks develop from the

borehole surface and grow outwards. After a short distance the number of the radial cracks decreases and usually only 4 to 8 symmetrically positioned cracks propagate (Field, 1971). However, the structure of the rock mass can affect the pattern of the cracks as observed by Trudinger and Worsey.

In the past two decades, a number of reduced-scale investigations were made in order to examine the effects of rock properties as well as geological discontinuities on rock fragmentation. A series of plexiglass model experiments were performed by Rinehart (1960) to determine the role the material strengths played during the fracturing process by explosion. He concluded that it is the net tensile stress that causes the separation of the material when it is over the tensile strength of the material.

Worsey and Chen (1985) conducted a program to investigate the effects of both the compressive strength and tensile strength of rock on the maximum successful borehole separation in rock splitting by high explosives. Their results show that only the tensile strength has a predominant influence on the successful splithole spacing.

It has also been recognized that geologic meso and micro structure is one of the most important factors affecting the result of a rock blasting operation (Ash, 1973; Worsey 1981; Worsey et al, 1981; Konya. 1984). Konya stated the following:

"Rock type, as well as it is relatively homogeneous, does not seem to be a significant factor for design consideration in pre-split blasting. Geologic structure is considerably more important."

Fourney et. al.(1979, 1980, and 1983) performed a series of blasting experiments with Plexiglas models to examine the mechanism of rock fragmentation in flawed and jointed materials. They found that fractures can be initiated at remote flaws by reflected stress waves from free surfaces and joints, and continue to drive the created fractures.

A similar program was carried out by Winzer et. al.(1980). It was concluded that fragmentation occurs by stress waves which reinitiate and open old fractures and initiate new fractures from existing cracks and other flaws in the rock.

So as to evaluate the effect of filling material, Singh and Sastry (1984) conducted a laboratory scale investigation with sandstone models. They found that the filled joints can, to some degree, influence the fracture pattern and the results of the rock fragmentation.

Another experimental study was made with emphasis on the influence of discontinuity filling materials on stress wave propagation. The magnitude of the stress wave will be somewhat attenuated when it transmits through discontinuities within the rock masses (Wild, 1977).

In 1983, a research program was performed with Plexiglas models by Bleakney et al. Their preliminary results indicated that discontinuity fillings had a significant effect on the results of splitting and that this line of research was worth further in-depth investigation.

As far as can be determined from searching the literature, no other work has been concerned with the effects of geological discontinuities on the splitting of rock.

B. MECHANICS OF ROCK SPLITTING

Energy release and transfer from an explosive detonation in a borehole to the surrounding rock is a complex process. It includes the forces from pressures acting over the borehole's surface area that accomplish the necessary work to cause sufficient stress conditions within the surrounding rock for fracture and displacement. There are two distinct and separate pressures produced by the explosive. The first is the dynamic stress waves generated by the explosive's detonation and the second one, which follows the first quickly, is that produced by the highly heated gases formed by the reaction of the explosive, which is commonly referred to as quasi-static gas pressure or borehole pressure (Ash, 1967; Britton and Konya, 1977; Worsey, 1981).

With regard to the respective roles played by dynamic stress waves and the quasi-static gas pressure in the splitting process, several contradictory theories explaining

the mechanics of the fracturing process exist in the literature. Basically, these theories can be divided into three general viewpoints. The first of them explains it from a dynamic standpoint. In this theory, stress waves from the detonation of high explosive charges are most responsible and the quasi-static gas pressure has little significance in the fracturing process (Duvall and Atchison 1957; Hino, 1965; Holloway, Fournery, and Barker, 1979, 1980, 1983). Cracks surrounding the explosive charge are produced when the tensile stresses induced by the incident stress waves and those reflected from free surfaces or existing flaws in the rock reach the tensile strength of the rock (Holloway et. al., 1980; Fournery et al, 1983).

By considering two adjacent boreholes fired simultaneously, Aso(1966) made a mathematical analysis of the rock splitting process in which strain pulses caused by stress waves from adjacent boreholes will superimpose at the midpoint and form a tension zone. When the tensile stress exceeds the tensile strength of the rock, splitting will initiate at the midpoint of adjacent boreholes, (see Figure 1). However, Kutter and Fairhurst (1967) have shown analytically that pre-split fractures do not initiate at the midpoint. Examination of typical pre-split fractures in rock also demonstrates that split fractures start from the borehole periphery and not the midpoint of the boreholes, (see Figure 2).

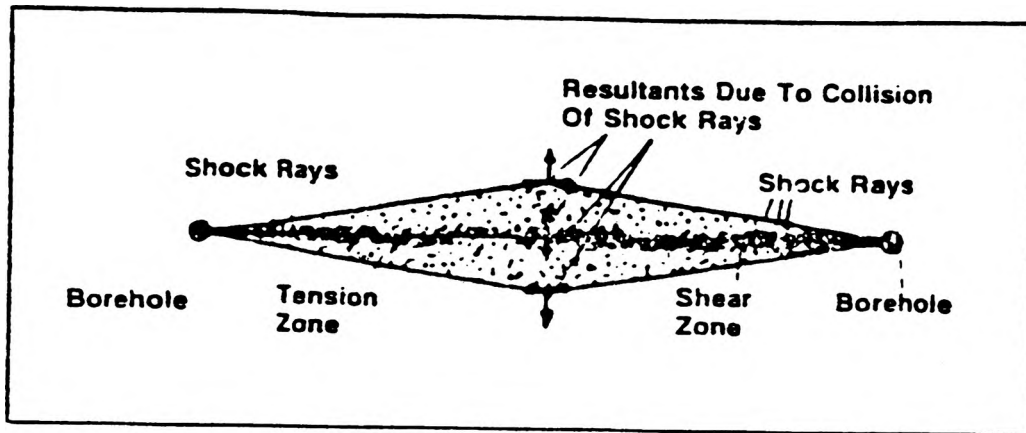


Figure 1: Principles of Pre-shearing
(after Aso, 1960)

Note: If holes are overloaded shear zone will extend to and beyond indicated tension zone.



Figure 2: Pre-split Fracture in Rock with
A Hole Spacing of 2.5ft.
(after Nicholls and Duvall, 1966)

Since the early 1970's, a series of Plexiglas model experiments have been made by Fourney, Holloway et al. (1979, 1981, 1983), incorporating high speed photography to examine the performance of the stress waves. Their results show that the time for completion of the split fractures is comparable with the transit times for stress waves between the shot holes, indicating the dynamic nature of splitting by high explosives. It has also been reported that fractures can be produced not only around the borehole area but they can also be initiated at remote flaws by the stress waves. Based on this finding, a joint initiated fracturing mechanism is suggested which implies that new fractures and cracks can be produced under the interaction between the existing cracks and the stress waves.

Contrarily, the second theory states that the process is similar to hydrofracture. The quasi-static pressure produced by the expanding gases, which is exerted over the borehole periphery, is the main force to create fracture planes (Kutter, 1967; Kutter and Fairhurst, 1967).

Britton and Konya (1977) performed an experimental investigation to determine the primary mechanism for breaking rock by varying the decoupling ratio of the explosive. They concluded that stress wave or shock energy cannot contribute significantly to rock breakage, and the primary force by which explosives break rock is gas pressure.

Porter and Fairhurst (1970) conducted a program to investigate the role of sustained borehole pressure following detonation in a blast. From the result of their study they concluded that under ideal conditions the cracks can be produced in the absence of stress waves and implied the dominant role of the quasi-static gas pressure in the fracturing process of rock splitting.

In 1985, Konya et al. made a series of full scale tests in granite using various presplit spacings. They successfully obtained the pre-split fractures with Pyrodex, a type of propellant which develops no dynamic shock waves in the rock and thus they concluded from their observations that the presplitting is caused by a hydraulic effect produced by the sustained gas pressure and that shock waves do not play any significant role in the breakage process.

The third and last theory, accepted by most people in recent years, states that both dynamic stress and gas pressure are responsible for the success of the explosive fracturing process (Kutter, 1967; Ash, 1967; Kutter and Fairhurst, 1967 and 1971; Worsey, 1981; Worsey et al., 1981). The initial high energy in the dynamic stresses initiates radial cracks around the borehole wall and then these cracks are extended by the pressure exerted by the expanding explosion gases within the borehole until a split is formed and opened by the gases escaping into the voids (Worsey, 1985). Worsey states the following:

"The dynamic component comprises initially a plastic headwave, decaying rapidly to form a radially expanding compression wave. ... The initial high energy in the wave is dissipated by local crushing at the borehole periphery and/or limited radial cracking parallel to the direction of maximum compression."

"As the headwave leaves the zone of the borehole, the borehole itself is pressurized by the build up of the gases which are a byproduct of the rapid combustion characterized by detonation. These exert a high quasi-static pressure on the borehole sidewall. The effect of this pressure is to induce compressive radial and, more important, tensile tangential stresses around the borehole which effectively open the existing limited length cracks produced by the dynamic wave."

In this work, it is generally accepted that a presplit is formed by the connection of fracturing from adjacent split holes, initiated by the dynamic shock wave and extended by the pressure exerted by expanding gases within the shotholes.

Until now, as far as can be determined from searching the literature, the vast majority of the rock fracturing and splitting theories are made under the assumption that rock is

a continuous material; little consideration has been given to the effect of geological discontinuities on performance of the rock splitting techniques, although some studies have been made on fragmentation in discontinuous materials.

III. DESIGN AND METHOD

The experiments discussed in this thesis were made utilising two borehole concrete and Plexiglas models. The concrete model experiments were concerned with investigating the effect of geological discontinuity conditions on the maximum successful spacing and the ability to split clearly between split holes. The discontinuities were designed in terms of their density, type of filling material and discontinuity width, as well as the profile roughness of the discontinuities.

The concrete used in this experimental work consisted of Portland cement, water and building sand in a proportion of approximately 1:1:4 at pouring. After four weeks of curing, the compressive strength and Brazilian disc tensile strength of the concrete were from 690 to 765 psi and from 235 to 267 psi, respectively. The longitudinal sound velocity was measured to be approximately 11,780 to 12,470 fps and the transverse velocity from 8,330 to 8,840 fps (see Appendix A).

The experiments utilizing Plexiglas models were made to examine the role of the dynamic stresses under varying discontinuity conditions, by optically examining the fringes linked with the stress propagation process and the fracturing processes using high speed photography.

Three general principles were applied to the design of the experiments in order to make the results applicable to

similar conditions in rock, taking into consideration physical property differences and scaling. First, the drill pattern, loading procedure and initiation sequence were designed as to generally simulate field pre-split blasts. Second, the split borehole diameter, the charge diameter and the explosive type were chosen to be similar and of the same order as used by others in similar experiments (for convenient comparison). Third, all possible attempts were made to assure that the discontinuity conditions were the only variables in the experiments, so that the results could be analyzed solely in terms of the effect of these variables.

A. EXPLOSIVE SELECTION

High detonation velocity explosives such as Primacord are considered more likely to cause overbreak. However, it has been shown that they are equally effective as low velocity explosives in producing a good split by proper decoupling of the borehole charges so as to damp the dynamic stresses caused by the detonation of the high explosives (Langefors and Kihlstrom, 1963; Britton and Konya, 1977; Simha, Holloway, and Fourney, 1979; Worsey and Chen, 1985).

Fifteen-grain PETN Primacord was selected to be the explosive for all the concrete model experiments in this study. The explosive PETN, being a common industrially manufactured high explosive product, is widely selected by experimentalists due to its consistent detonation velocity

regardless of charge diameter and its ability to propagate energetically at small diameters. The charge density of this Primacord is 15 grains per foot and its detonation velocity is from 6,700 to 7,000 meters per second.

For the Plexiglas model tests, Reynolds Industries RP-80 detonators were chosen for the explosive borehole charges after preliminary experiments using PETN Primacord failed to provide adequate results, due to the extra light from the blasting cap located outside of the blasthole and the considerable smoke from the detonation of the primaline resulting from its thick plastic sheathing. The RP-80 detonator contains 78 mgs of PETN as the initiating explosive and 124 mgs of RDX as the output explosive. The diameter and the total length of the detonator are 0.28 and 0.70 inch, respectively.

B. BLASTHOLE DIMENSIONS

1. Concrete Test Models. As stated before, explosive charges for rock splitting boreholes are normally decoupled. As the diameter of the PETN Primacord is 0.145 inch, the borehole diameter for the concrete models was chosen to be 3/8 inch so as to avoid severe crushing around the boreholes by the explosive (Atchison, 1961) and a nominal decoupling ratio of 5.2 was achieved, as used by Worsey and Chen (1984) in their laboratory-scale rock splitting program, which falls into the range of field practices (Langefors, 1966; Mellor, 1976).

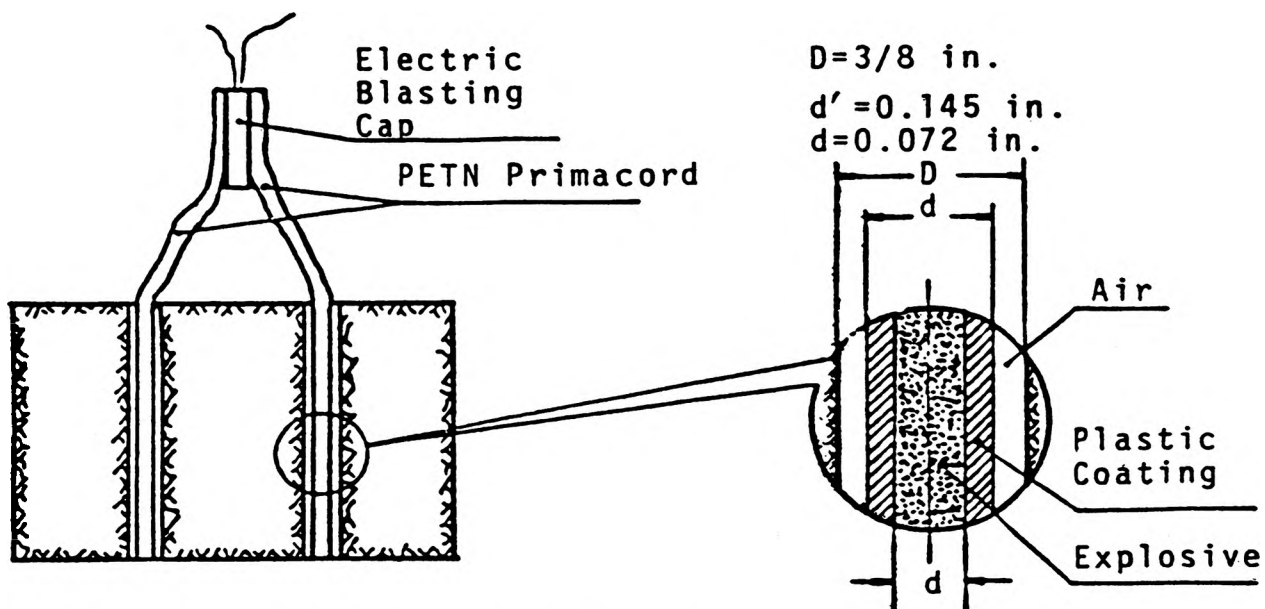


Figure 3: Concrete Model Test Borehole Explosive Loading Structure

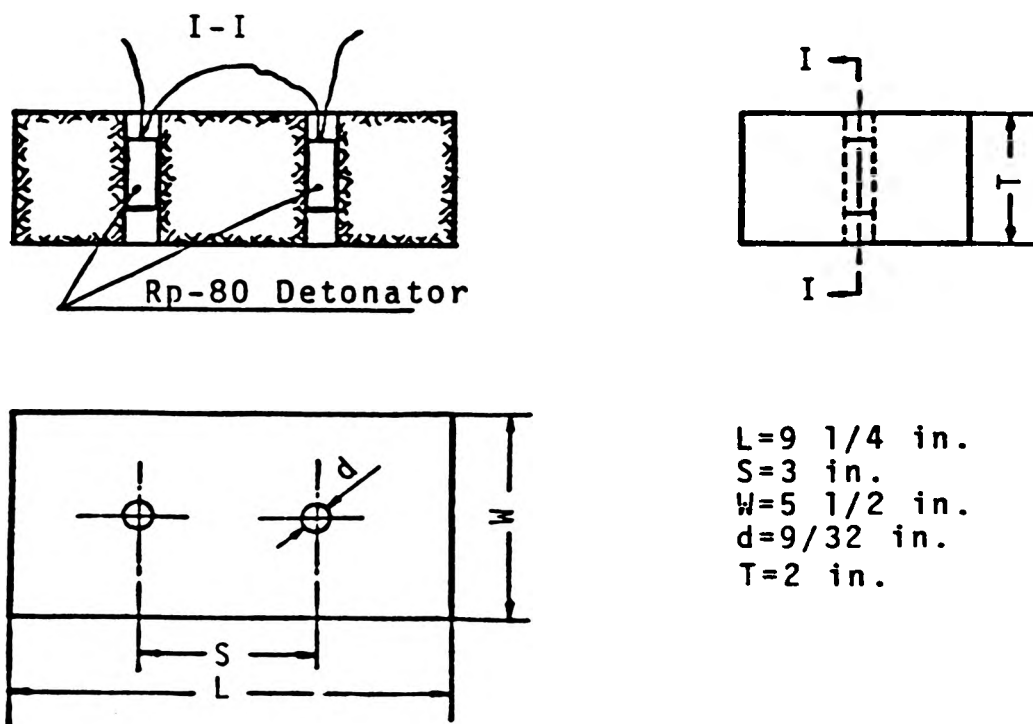


Figure 4: Plexiglas Model Test Borehole Explosive Loading Structure

Boreholes were drilled completely through in each of the test models (see Figure 3).

2. Plexiglas Test Models. Since the purpose of the Plexiglas model test study was to optically analyze the stress field patterns under different simulated geological discontinuity conditions, and then study the effect of the geological discontinuities on the rock splitting mechanics qualitatively, the decoupling degree was not considered important. Knowing that the diameter of the RP-80 detonator, used as the explosive charge for the Plexiglas models, is 0.28 inch, the borehole diameter was chosen to be $9/32$ (decimal equivalent of 0.28) inch. Similarly to the concrete model tests, the boreholes were drilled completely through the Plexiglas (see Figure 4).

C. LOADING PROCEDURE AND INITIATION

1. Concrete Model Tests. Loading of the boreholes was as follows. For the concrete model tests, the Primacord was first cut to strings of equal length L , the sum of the borehole depth, t , and s , the section of the primaline left outside of the borehole for convenient connecting of the charges for the model. Then, one end of the length of Primacord was loaded to the bottom of the borehole while the other end was bonded to an electric blasting cap located outside of the borehole (see Figure 3).

Precise simultaneous initiation was used for the concrete model test blasts and accomplished by connecting the ends of the two strings of precisely equal length of PETN Primacord and the initiating blasting cap together outside the boreholes. For these tests, stemming of the borehole collar was not performed.

2. Plexiglas Model Tests. For the Plexiglas model tests, RP-80 detonators were used as the explosive charges. Each borehole was loaded with one of the detonators with the detonator leg wires extended outside.

Similarly to the concrete model tests, simultaneous initiation was used. This was accomplished by connecting the two instantaneous detonators for each test blast in series (see Figure 4). In this way, the two splitting boreholes for each test would be fired simultaneously since the RP-80 detonators were identical and their timing characteristics well defined (nominal function time < 3.0 microsecond with a standard deviation of 0.125 microsecond).

In order to avoid stemming material blowing out and obscuring clear pictures of the stress pattern and the fracturing process during the dynamic event, no stemming was used in the Plexiglas model tests.

D. TEST MODEL DIMENSIONS

1. Concrete Test Models. As stated before, this investigation is concerned with rock splitting problems

inherent in pre-split blasting applications to discontinuous rock masses. It is important and necessary that the specific features involved in field pre-split blasting operations be known and simulated properly in the dimensional design of this experimental work.

For field pre-splitting, boreholes are drilled along the desired perimeter of the excavation with a smaller spacing than that used for bulk blastholes and explosively loaded with a decoupling ratio ranging from approximately 2 to 5. Another characteristic of the technique is that the pre-split boreholes are fired just before the bulk blast holes, which is implied by the term "pre-splitting". The free surface of the rock mass can be a considerable distance away from the pre-split holes. Tensile stress reflected from the free surface is considered to have little effect, if any, on the rock splitting process at the line defined by the pre-split holes.

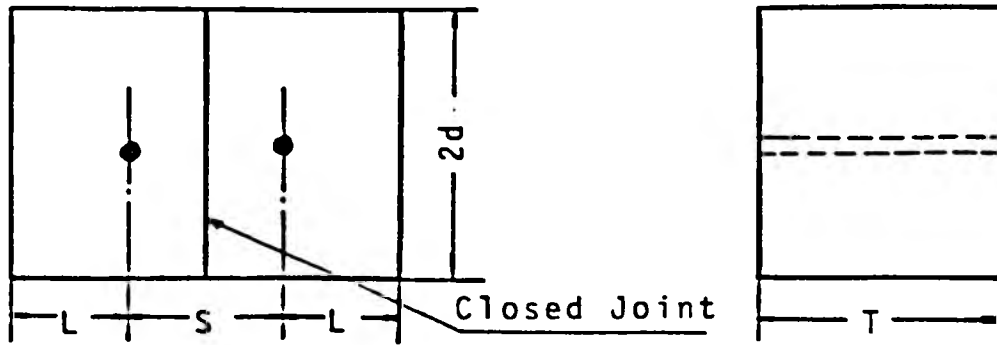
As an effort to make the experiment consistent with these field rock splitting conditions, the distance d from the desired split line to the side free surfaces of the model should be at least as large as half of the maximum successful spacing so as to avoid fracturing and relief at the side surfaces before a possible split is induced. Stress wave propagation will be diametrically identical, providing the medium is homogeneous and continuous. The time required for the wave coming out from the borehole and then being reflected, if possible, back to the borehole area must be

longer than that for the stress wave fronts to move and reach the adjacent boreholes. Noticing that the maximum successful spacing for a concrete medium and similar experimental configuration was 4 inches (Worsey and Chen, 1986), the distance d was predetermined to be 5 inches. In addition, wave traps were used to reduce the unwanted reflections, which are discussed in detail in Appendix C.

After determining from preliminary tests that the maximum successful split-hole spacing for continuous concrete was 4 1/2 inches, the distance, d , was assigned to be a constant of 5 inches which satisfies the requirements discussed above (see Figure 5).

In field pre-splitting practices, free surfaces are usually so far from the boreholes that they can have little, if any, effect on the formation of the split. For the model tests of this experimental work, a cratering effect at the end surfaces of the test model can be expected, which most likely has an influence on the splitting between the split holes. Based on this consideration, the distance, L , from a borehole to the near end surface of the test model, was chosen to be 2 3/16 inches for each of the concrete models, which is close to half of the maximum spacing for continuous concrete models.

Another factor is the borehole depth. Since the boreholes were drilled completely through each of the concrete models, this was 6 inches.



T=6 in.
 d=5 in.
 L=2 3/16 in.

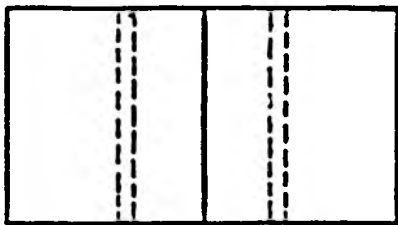
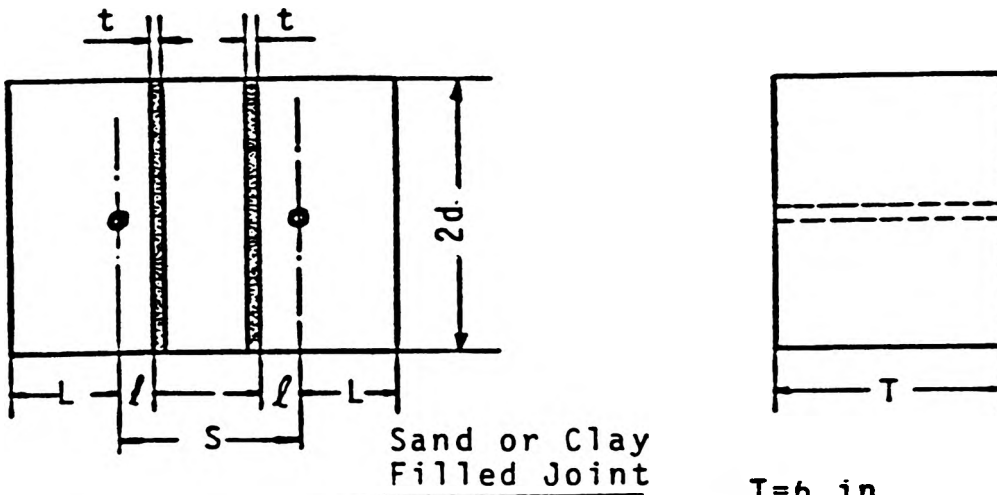


Figure 5: Dimensions of Concrete Model With One Discontinuity



T=6 in.
 $\phi=1 \frac{3}{8}$ in.
 d=5 in.
 t=1/16, 1/8, 1/4 in.
 L=2 3/16 in.

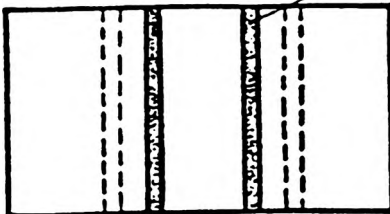


Figure 6: Dimensions of Concrete Model with Two Discontinuities

For the two-joint model tests, the distance from a borehole to its nearby discontinuity was a constant of $1 \frac{3}{8}$ inches. Borehole spacing was subjected to change by adjusting the width of layer between discontinuities for different filling width conditions.

2. Plexiglas Test Models. In order to make a good comparison and provide contrast among the stress field patterns from these tests as well as their development with time under different conditions, the borehole spacing was kept at a constant 3 inches for each test model. Total model length and width were 9.25 and 5.5 inches, respectively, in which the distances d and L were $3 \frac{1}{8}$ and $2 \frac{3}{4}$ inches, respectively, so as to avoid any end surface cratering effects and stress wave reflection effect from the side surfaces of the test models (see Figure 6). Wave traps were also used with a width being approximately 5.5 inches which was consistent with the Plexiglas model width. In the tests with two discontinuities, the distance from borehole center to the closest discontinuity was kept at a constant value of one inch. Filling materials were used within the prepared discontinuities for the two joint test models.

As the Plexiglas model tests were made to visualize the dynamic stress wave propagation process, the thickness of the Plexiglas models should be limited in order to achieve clear fringe patterns which represent the stress distribution within the model. This thickness was chosen to be 2 inches and

these Plexiglas model tests were considered to be two dimensional and thus the test result was more qualitative rather than quantitative.

For models with only one joint, the joint was located midway between the two boreholes. Similarly, for models with two discontinuities, each discontinuity was located one inch away from the borehole closest to it. Borehole spacing was controlled by varying the width of the layer between the two discontinuities for different filling widths. The discontinuities were formed by cutting the Plexiglas block into smaller blocks of designed size. The cut faces were machine smoothed. And then boreholes were drilled and the original blocks were reassembled as test models.

E. DISCONTINUITIES AND FILLING CONDITIONS

Joints and other geological fissures present in a rock mass can have a considerable influence on rock splitting. They can be characterized by a number of factors. These factors are discussed below and were simulated through the design of the model experiments.

1. Joint Set Number and Orientation. Joints are most likely to occur in rock under tectonic stresses of sufficient amplitudes. Depending on the history of the tectonic stresses within the area concerned, one, two, three or even more sets of joints may occur. For simplicity, only the condition of one joint set was simulated and studied in these experiments.

Obviously, joint frequency, i.e., the number of joints existing within a certain distance can vary from one site to another. As an effort to find out how the joint frequency affects the result of rock splitting operations, one joint and two joints were made midway between two adjacent boreholes on concrete models, (see Figures 5 and 6). For the later case, the distance between the two joints was varied from one test to another until the maximum successful spacing was found while all the other factors of the model design were kept constant.

As the effect of orientation of geological discontinuities has already been thoroughly studied (Trudinger, 1973; Worsey, 1981), the simulated joints were all oriented perpendicular to the desired split plane.

2. Joint Extent and Width. In field conditions, joints and other discontinuities vary in extent, with a wide range. This aspect of the problem was simplified in this work and only the situation in which continuous joints completely run through across the desired split plane of the test models was studied. Tight joints, and joints of 1/16 inch, 1/8 inch and 1/4 inch width were used with different filling materials.

3. Filling Materials. The type of filling materials within discontinuities may have a considerable influence on rock fracturing and splitting operations. The strength of a rock mass and the stresses induced in the rock mass by the explosive are dependent upon the filling conditions of joints

and/or other geological discontinuities (Wild, 1977; Singh and Sastry, 1984, Bleakney et al., 1983). Energy carried by the dynamic stress waves can be partly consumed over the joints to some degree depending on the width and the impedance of the filling material.

Siliceous filling, clay filling and tight joints are the three most common situations found in field. Therefore, for this model scale research project, clay and fine siliceous sand were selected for the discontinuity filling materials. Physical properties of the two filling materials used are given in Appendix B.

F. INSTRUMENTATION OF PLEXIGLAS MODEL TESTS

All the Plexiglas model splitting tests were fired in the blasting chamber located in the Explosives Research Laboratory at the Rock Mechanics and Explosives Research Center of the University of Missouri-Rolla.

1. Properties of Plexiglas. The Plexiglas used for this work is manufactured by Rohm and Haas, Philadelphia. It is shatter resistant and transparent. It can be sawed, drilled and machined like wood or any soft metal without changing its properties.

Plexiglass is a thermoplastic material having a specific gravity of 1.18 to 1.19. It is solid up to a temperature of approximately 200 degree Fahrenheit and has a hardness of 2 to 3 on the Mohs scale of hardness. Its static tensile strength

is between 7,000 and 8,000 psi, with an elongation at failure of 5 to 15 percent (Haas,1963).

The ultrasonic velocity of Plexiglas was measured with a pulse generator and oscilloscope. The longitudinal wave velocity was found to be 9,070 fps. and the transverse wave velocity 4,455 fps.

Plexiglas is considered to be a good material for studying fracturing phenomena since it is a transparent and birefringent material. When polarized light is traveling through a two dimensional Plexiglas plate in a plane stress condition, the stress field within it can be visualized as colored fringes.

Stress wave propagation within test models is a dynamic process. The material at a certain distance away from the borehole is oblivious of neighboring events and therefore no fringes are induced until the stress waves arrive. Thus, the Plexiglas material offers an opportunity to optically analyze the stress wave initiation and propagation processes and the fracturing process during the splitting event, with the use of the technique of high speed photography.

2. Description of Polariscopes. A polariscopes is a set of optics which is used to make the stresses occurring in a birefringent material visible as colored fringes when the material is illuminated by polarized light.

Since the Plexiglas model test blasts were made to analyze the stress wave propagation and the fracture

initiation and extension, only the isochromatics were needed, which are representative of the amplitude of principal stress difference (Hansen, 1985). This is furnished by the standard crossed circular type of the polariscope.

The polariscope used in this work consisted of the following elements in the order: light source, polarizer, first quarter-wave plate, test model, second quarter-wave plate, and analyzer which were arranged as shown in Figure 7. The diameter of the polariscope was 14 3/4 inches.

The axes of the polarizer and analyzer are perpendicular to each other, likewise the fast axes of the two 1/4 wave plates are also perpendicular. The fast axis of the first 1/4 wave length plate is set to be 45 degrees away from the axis of the polarizer. The light emerging from the polarizer is single plane polarized. The first quarter-wave plate is used to circularly polarize the plane polarized light into two components which are perpendicular to each other and have a constant phase shift with respect to each other. If the light coming to the first quarter-wave plate is monochromatic and the plate was designed exactly for this light, this phase shift will be exactly of quarter-wave length. Otherwise, the light will be elliptically polarized and a slight shift in the isochromatics will be induced as a result. However, as only the pattern of the stress field during the dynamic process is required, the light component is not crucial and a monochromatic light source is not crucial.

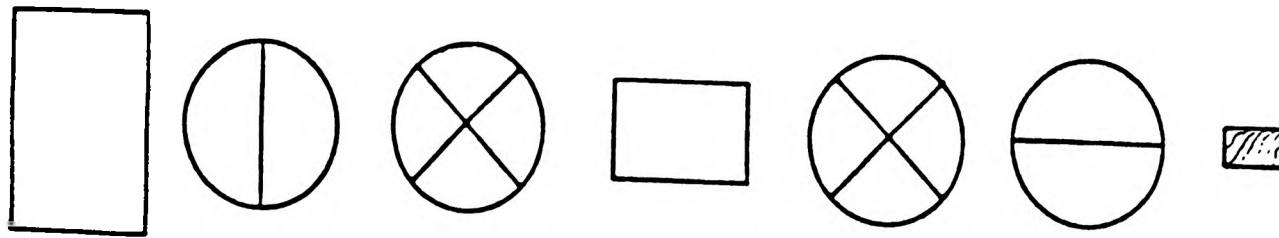
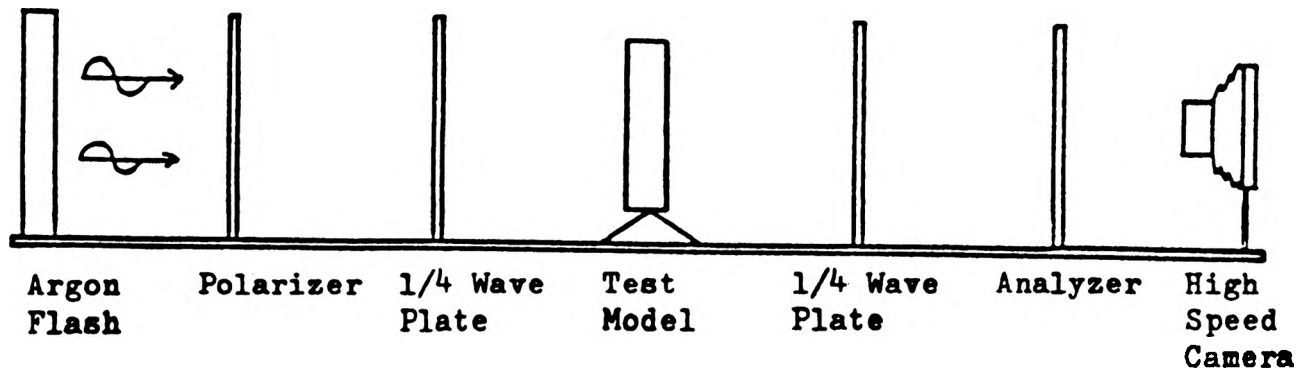


Figure 7: Arrangement of Components of the
Circular Polariscope
(after Hansen, 1985)

An Argon flash was used as the light source in order to provide sufficient light intensity and induce an appropriate illuminance on the 2 inch thick Plexiglas test models. This Argon flash consisted of a paper cardboard box one foot high, one foot wide and three inches in depth. The front cover of the box was made of a thin transparent plastic sheet. A piece of 1/16 inch thick Detasheet was attached to the back of the argon flash box. An electric detonator was used to initiate the Detasheet. Just prior to the test, the Argon gas was filled into the flash box through a small tube. Argon gas produces high intensity light under the stimulation of the high energy liberated by the detonation of the Detasheet and/or an electric cap. Since the propagation of the Detasheet initiated stress waves in the Argon is slightly above the velocity of sound transmission, the light duration can be easily controlled by the depth of the Argon flash box. According to Tyler (1985), the light intensity from an Argon flash is proportional to the cross section area of the flash.

For each test blast in the Plexiglas models, an Argon flash was positioned in the chamber with its face towards the safety glass window, the window A as shown in Figure 8. The light path was to the following elements in sequence: safety glass window A, reflection mirror 1, reflection mirror 2, polarizer, safety glass window B, reflection mirror 3 in the blasting chamber, the test model, safety glass window C, the analyzer, and finally the lense of the high speed framing camera (see Figure 8).

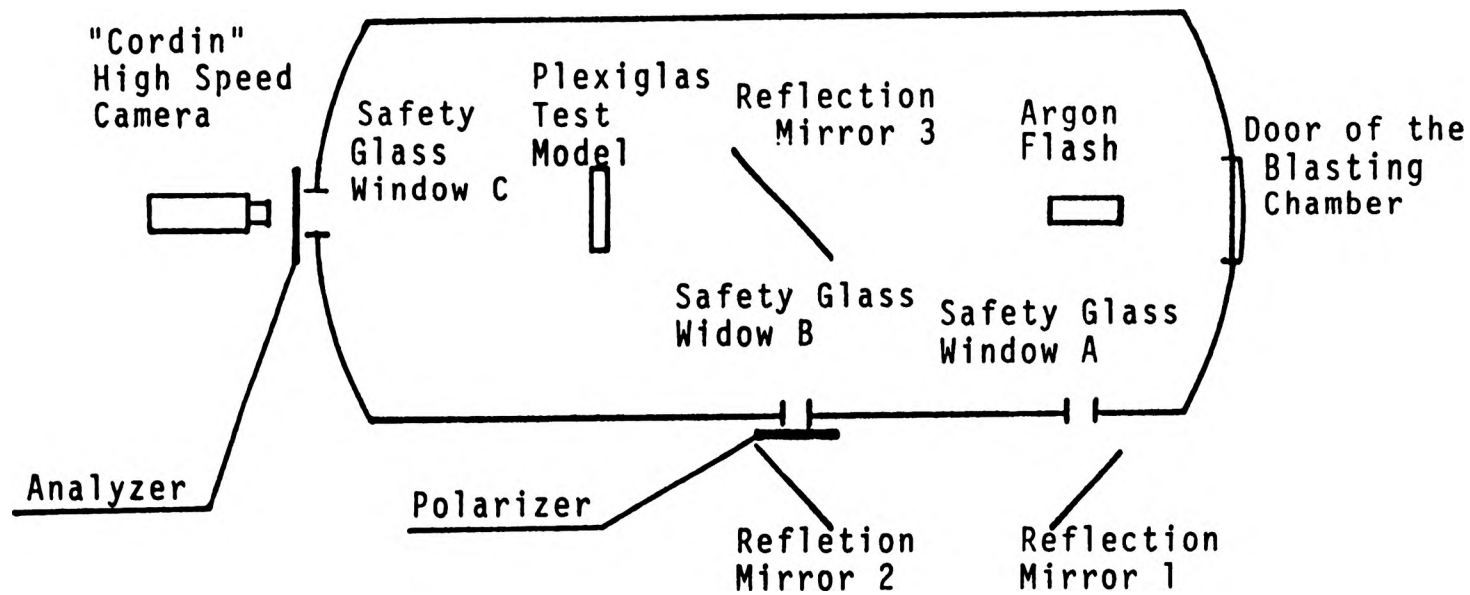


Figure 8: Arrangement of the Instruments for High Speed Photography of Plexiglass Model Tests

3. High Speed Camera. The explosive blasting event is a complex process and the period of time of this event is so short that the details of the phenomena occurring cannot be observed by normal photographic means. The high speed photographic technique, which was utilized in the Plexiglas model tests, offers the chance to eliminate this problem (Bair, 1959; Fourney et. al., 1979, 1980, 1983). Stress waves are observed as fringes in the two dimensional Plexiglas models. Fracture initiation and propagation may also be visualized from the pictures taken by the high speed framing camera.

The high speed camera was of a synchronous, framing type, manufactured by the Cordin Company of Salt Lake City, Utah. As the turbine in the camera rotates the mirror attached to the turbine reflects the images of the object, the Plexiglas model of the blast test, to the stationary film via relay lenses and field flatteners. The high speed framing camera used has a maximum safe framing rate of 1.25 million frames per second and a film capacity of 26 frames.

There are two critical factors in the utilization of the high speed camera. One is the active exposure time which is related to the mirror period determining the framing rate, and the other is the synchronizing of the blast event with film exposure time and the initiation of the Argon flash which serves as the light source and ultimately exposes the film.

The active exposure interval of the Cordin synchronous framing camera is approximately one eighth of its mirror period, which is determined by the design of the camera. From preliminary experiments, it was found that a mirror period of 625 microseconds was appropriate to cover the phenomena of interest that occurred during the event. The 625 microsecond mirror period represents an interframe period of 2.5 microseconds and a total exposure time of approximately 78 microseconds.

The synchronization of the explosive blasting event with the camera's active writing time and the initiation of the Argon flash is facilitated with a mirror position sensor in the camera, which detects when the mirror attached to the turbine is $1/10$ mirror period ahead of exposing the first frame, and the synchronization control system of the Cordin high speed camera (see Figure 9). In order to protect the polariscope from explosion of the test blasts and the firing of the Argon flash, the polariscope was positioned outside the blasting chamber. The reflection mirrors were required and used to direct the light for this particular situation. Since only the pattern of the stress wave front and the possible fracture process caused by explosion within the test models were of interest, the possible polarization effects of the mirrors were ignored.

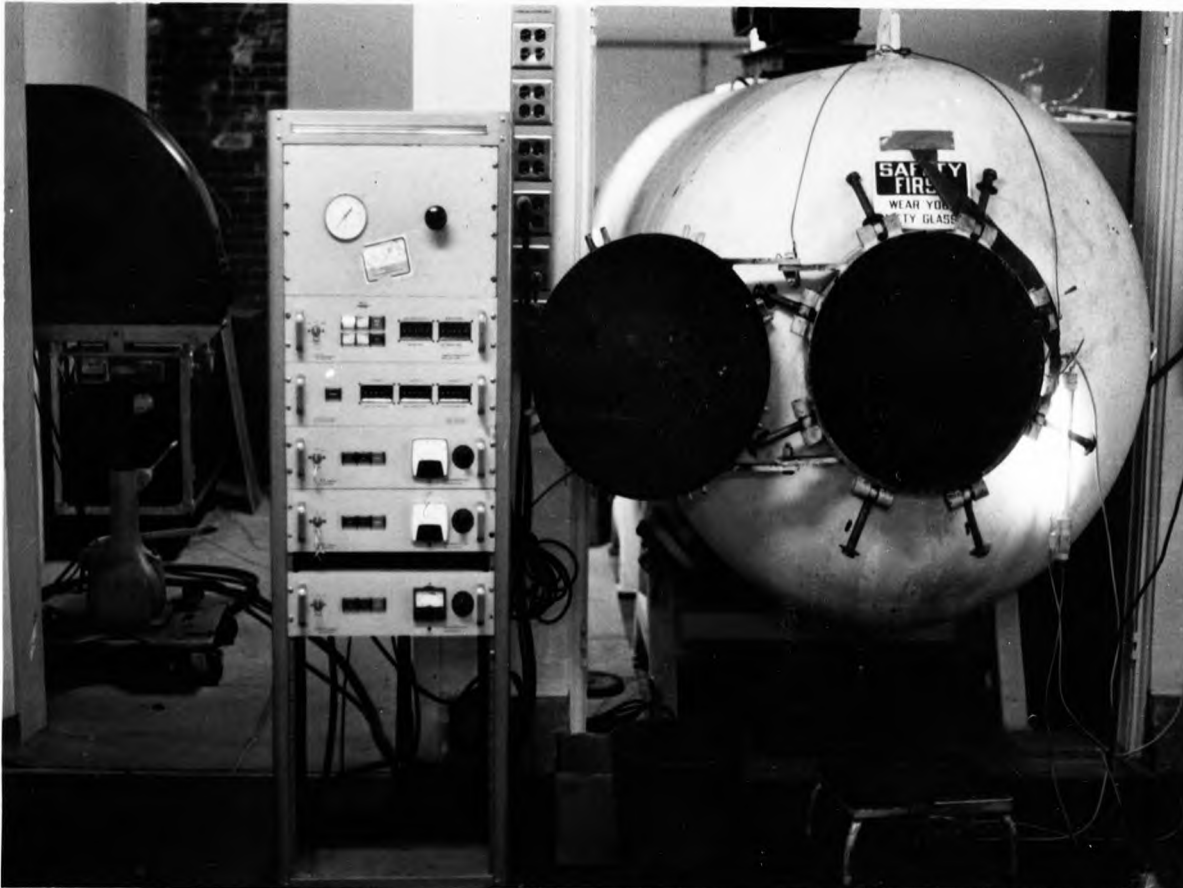


Figure 9: Blasting Chamber and "Cordin" Synchronization
Instrument for the High Speed Camera

IV. RESULTS AND DISCUSSION

As stated before, this experimental research work was composed of two phases, the first carried out using concrete model tests to examine the effect of the simulated geological discontinuities on rock splitting performance, the second using Plexiglas models, taking advantage of the specific photoelastic properties of the material, and high speed photography to optically analyze the high speed phenomena occurring during explosive rock blasting.

A. CONCRETE MODEL TESTS

1. Maximum Successful Split-hole Spacing for a Continuous Concrete Medium. Rock masses found in the field are commonly separated by different geological discontinuities which have a considerable effect on the performance of blasting.

For the concrete modal scale study discussed in this thesis, the maximum successful spacing of split holes for continuous concrete models needed to be found, in order to serve as a base for comparison and analyses with those of different simulated geological discontinuity model tests of the same medium.

Before the first test model was designed, it was noticed that, according to Worsey and Chen (1986), the maximum successful spacing, for the continuous concrete they used,

was four inches. And, it was also noticed that the compressive and tensile strengths of the concrete were both close to, but higher than those for the concrete used in this work. Based on this information, the split-hole spacing for the first test model was designed to be five inches in an attempt to determine the maximum successful spacing for the continuous concrete. Results of this test showed that no continuous and clear split plane was achieved while only some micro fractures were apparent along the centerline of the model, (see Figure D-1).

Following the first test, adjustment was made and the split-hole spacing was reduced to 4.5 inches for tests C-2 and C-3. Although a continuous and clear split plane was found in test C-2, it could not be regarded as a success since overbreak, i.e., severe fracturing, occurred. By post-test examination of the test model, it was found that the model was not as dry as expected, which could have reduced the strength of the concrete and caused the overbreak. A clear and continuous split was found in test C-3, (see Figure D-2). Another two tests, which are listed in Table I as tests C-4 and C-5, were made with split-hole spacing of 4.25 and 4.5 inches, respectively. Overbreak occurred in test C-4 and successful splitting was achieved in test C-5. It was concluded that the maximum successful split-hole spacing for this continuous concrete medium was 4.5 inches.

TABLE I
 DATA OF THE MAXIMUM SUCCESSFUL SPLITHOLE
 SPACING FOR THE CONTINUOUS CONCRETE

Test No.	S(in.)	d'(in.)	d(in.)	D(in.)	R	Result
C-1	5.0	0.145	0.072	3/8	5.2	Failure
C-2	4.5	0.145	0.072	3/8	5.2	Failure
C-3	4.5	0.145	0.072	3/8	5.2	Success
C-4	4.25	0.145	0.072	3/8	5.2	Failure
C-5	4.5	0.145	0.072	3/8	5.2	Success

Note: S is the splithole spacing;
 d' is the diameter of the Primacord;
 d is the explosive charge diameter;
 D is the split-hole diameter;
 R is the ratio of D to d.

2. Effect of Discontinuity Frequency. Experiments for this section of the work consisted of continuous medium tests, one closed-up joint model test, and two closed-up joint model tests with the joints being located midway between the split holes. For the two-joint model tests, each joint was located $1 \frac{3}{8}$ inches away from its nearer borehole. No filling was used for the simulated joints of the test models in this part of the work.

a. Single-Closed-Joint Model Tests. This part of the model scale study consisted of three tests. The difference between these test models and those discussed above is that they were made from the second mix of the concrete, where the compressive strength and the tensile strength were to some degree lower than that of the first mix (see Appendix A).

A borehole spacing of $4 \frac{1}{2}$ inches was selected for the first test. This test was a success (see Table II and Figure D-3). A 5.25 inch spacing was used in the test C-7 after the first test. No split, and only micro cracks were produced (see Figure D-4). Test C-8, therefore, was carried out with a split-hole spacing of $4 \frac{7}{8}$ inches which is close to the average of those for the former two tests. Although some micro cracks were created around the split holes, this test was a failure and no split was formed along the splitholes.

The number of tests performed up till this point would be normally insufficient to make positive conclusions. However, it can be said from results of these tests that the maximum

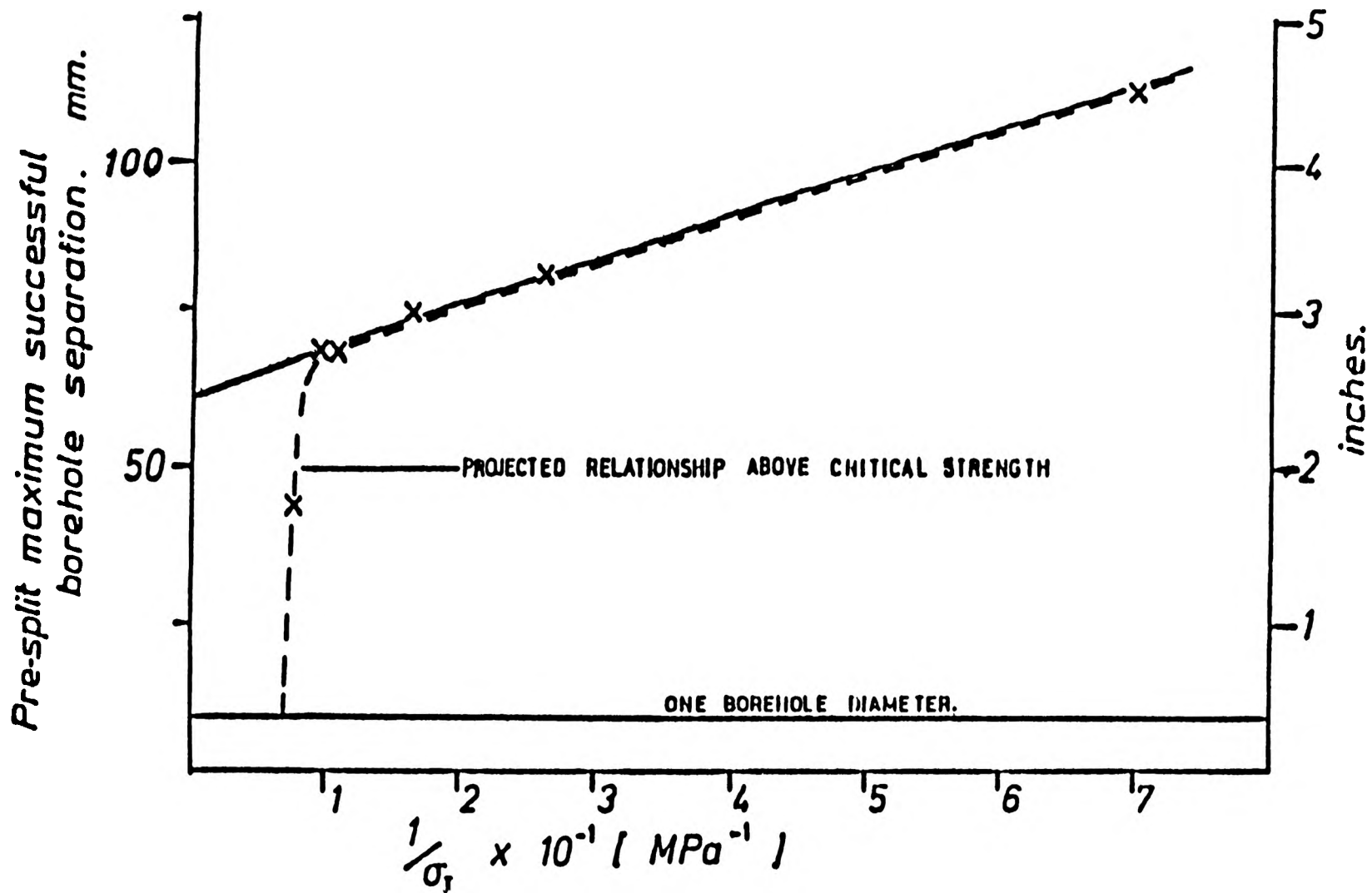


Figure 10: The Inverse Relationship between Maximum Successful Split-hole Spacing and Rock Tensile Strength (after Worsey, 1981)

successful split-hole spacing is around 4 1/2 inches although no further tests were made due to a shortage of the prepared concrete.

It can be assumed that the maximum successful split-hole spacing is inversely proportional to the tensile strength of the material (see Figure 10). Knowing that the tensile strength for the two mixes of concrete were 267 and 235 psi, respectively, the result of 4 1/2 inch spacing is equivalent to about 4 inches if they had been made on the first mix of concrete.

b. Two-Closed-Joint Model Tests. A total of five model tests were made with each having two joints. They were all cast from the first mix of concrete.

Test C-9, in which borehole spacing was 4 3/8 inches, resulted in a failure and no split was achieved. Therefore, the spacing was reduced to 3 3/4 inches in the following two tests, tests C-10 and C-11. In test C-10, a split was created and the split line was not straight along the center line of the model (see Figure D-21). Test C-11 was a success.

Another test, test C-12, with spacing of 3 7/8 inches was carried out and the result was a success (see Figure D-6 and Table II). However, a test with a spacing of 4 inches was made later and it was found that only minimal cracks were produced along the center line of the test block. Although test C-10 represents an exception, it is considered reasonable to conclude that the maximum successful split-hole spacing under this given condition is approximately 3 7/8 inches.

TABLE II
DATA OF CLOSED JOINT MODEL TESTS

a. One Closed Joint

Test No.	S(in.)	d'(in.)	d(in.)	D(in.)	R	Result
C-6	4 1/2	0.145	0.072	3/8	5.2	Success
C-7	5 1/4	0.145	0.072	3/8	5.2	Failure
C-8	4 7/8	0.145	0.072	3/8	5.2	Failure

b. Two Closed Joints

Test No.	S(in.)	d'(in.)	d(in.)	D(in.)	R	Result
C-9	4 3/8	0.145	0.072	3/8	5.2	Failure
C-10	3 3/4	0.145	0.072	3/8	5.2	Failure
C-11	3 3/4	0.145	0.072	3/8	5.2	Success
C-12	3 7/8	0.145	0.072	3/8	5.2	Success
C-13	4	0.145	0.072	3/8	5.2	Failure

Note: S is the splithole spacing;
d' is the diameter of the Primacord;
d is the explosive charge diameter;
D is the split-hole diameter;
R is the ratio of D to d.

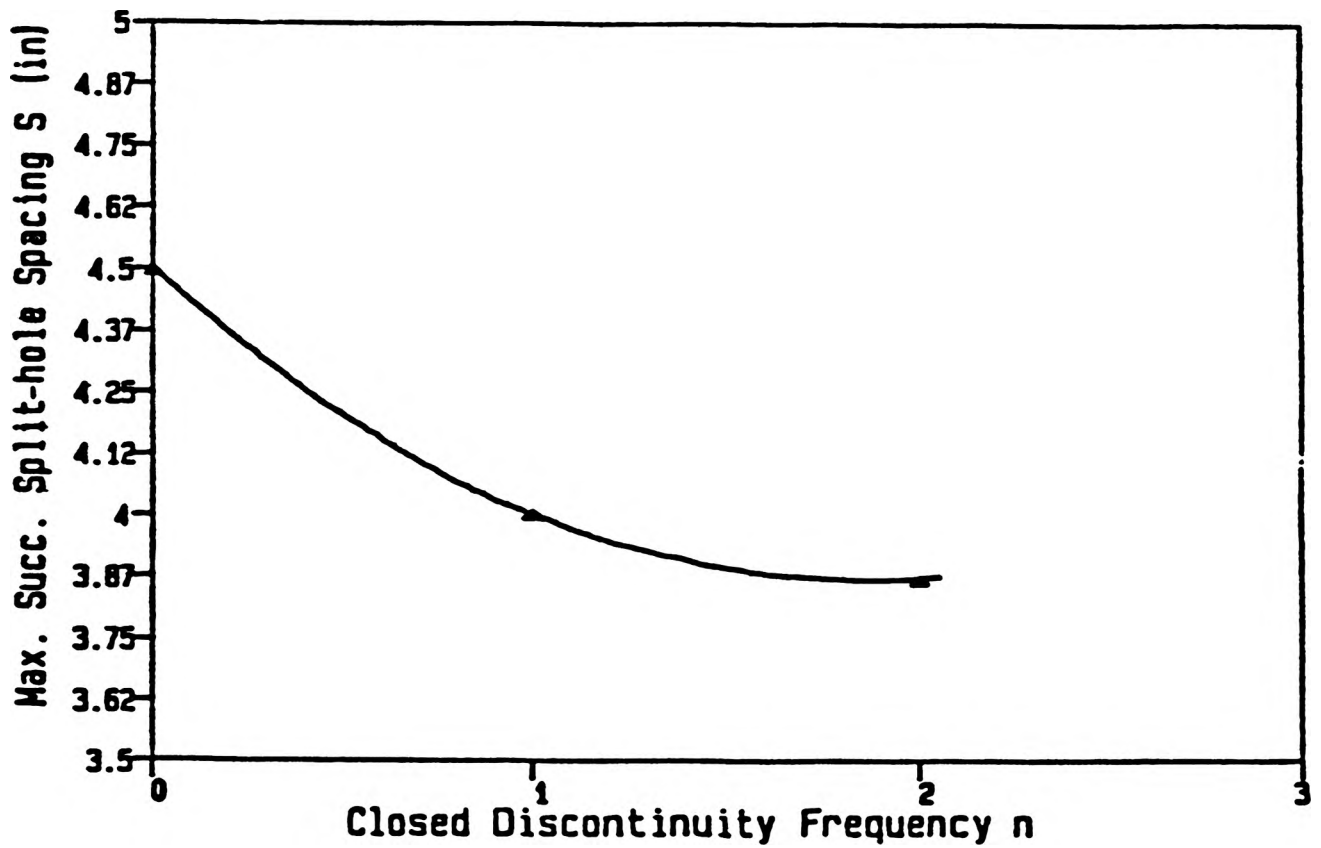


Figure 11: Maximum Successful Split-hole Spacing S_m
vs. Closed Discontinuity Frequency n

The data of the maximum successful split-hole spacing and the correspondent discontinuity number are listed in Table V (p.55) and plotted in Figure 11. A tentative correlation between these two variables is made which is represented by the following:

$$S_m = 0.1875n^2 - 0.69n + 4.5$$

in which

S_m is the maximum successful split-hole spacing, in. ;
 n is the number of discontinuities between the two
 split holes, $n=0,1,2$.

3. Effect of Filling Materials. As stated before, siliceous material and clay are the two most common discontinuity fillings found in field rock masses. Based on this consideration, fine siliceous sand and clay was chosen to be the filling materials for the simulated geological discontinuities applied in this section of model splitting tests. As an effort to simulate field filling conditions, the sand and clay were added with approximately 10 and 15 per cent of water before setting up each test model. For each of the tests, two joints were used and located midway between the two splitholes while the distance of the two joints was subject to adjustment until the maximum successful split-hole spacing was determined. The concrete blocks were all cast from the first mix of concrete.

a. Sand Filling.

1) Joint Filling Width $t=1/16$ Inch. Data and results of the tests are given in Table III. The first two tests, tests C-14 and C-15, were carried out with the same spacing of 4 inches. The two tests both resulted in failure and no split was created within the joint isolated section of the model (see Figure D-7). The split-hole spacing for test C-16 was designed to be $3\ 7/8$ inches by reducing the width of the middle section of the model to $1\ 1/8$ inches. In this test, a success was achieved while slight cratering, i.e., the radial fracturing within the region specifically from boreholes to the nearby discontinuities, occurred from the boreholes toward the joints (see Figure D-8). The same design was applied to test C-17 and the result was almost the same. No more tests were made, and $3\ 7/8$ inches was considered to be the maximum successful split-hole spacing for the designed condition.

2) Joint Filling Width $t=1/8$ Inch. These tests were similar to those described above differing only by that the discontinuity width t was increased to $1/8$ inch. The design and results of the tests are given in Table III.

Four inches spacing was used in test C-18 with the width of the middle section of the test block was $1\ 1/4$ inches. No split was produced through the middle section (see Figure D-9). Test C-19, in which the split hole spacing was reduced to $3\ 3/4$ inches, was not effective since the two end pieces of the

model were made, by a mistake, from the second mix concrete, while the middle section of the test model was cast from the first mix concrete. However, although no successful splitting occurred, the result of severe cratering towards the two discontinuities can be accounted for by the comparatively low strength of the two end concrete parts of the model (see Figure D-22). Test C-20 was carried out with the same dimension design as that for test C-19. This test was a success but, the split within the middle section was not in the center line of the model (see Figure D-10). No obvious defect was found in this section by post-test examination. For test C-21, the split-hole spacing was increased to 3 7/8 inches. This test was not a success while minor cratering occurred. Based on the results of the tests, it can be concluded that the maximum successful spacing when the discontinuity width is 1/8 inch was roughly 3 3/4 inches.

3) Joint Filling Width $t=1/4$ Inch. Split-hole spacing for test C-221 was 4 1/4 inches and the width of the middle section was designed to be 1 1/2 inches (see Figure D-11). Since the result of this test was a failure, the spacing was reduced to 3 3/4 inches for the following test, test C-23. This test was again a failure and no split was achieved. Test C-24 and consequently test C-25 were then made with the same split-hole spacing of 3 5/8 inches. A continuous and clear split fracture was obtained in both tests (see Figure D-12). The split-hole spacing was then increased to 3 3/4 inches for

TABLE III
DATA OF SAND-FILLED, TWO-JOINT CONCRETE MODEL TESTS

a. Sand Filling Width $t=1/16$ in.

Test No.	S(in.)	d'(in.)	d(in.)	D(in.)	D/d	Result
C-14	4	0.145	0.072	3/8	5.2	Failure
C-15	4	0.145	0.072	3/8	5.2	Failure
C-16	3 7/8	0.145	0.072	3/8	5.2	Success
C-17	3 7/8	0.145	0.072	3/8	5.2	Success

b. Sand Filling Width $t=1/8$ in.

Test No.	S(in.)	d'(in.)	d(in.)	D(in.)	D/d	Result
C-18	4	0.145	0.072	3/8	5.2	Failure
C-19*	3 3/4	0.145	0.072	3/8	5.2	Success
C-20	3 3/4	0.145	0.072	3/8	5.2	Failure
C-21	3 7/8	0.145	0.072	3/8	5.2	Failure

c. Sand Filling Width $t=1/4$ in.

Test No.	S(in.)	d'(in.)	d(in.)	D(in.)	D/d	Result
C-22	4 1/4	0.145	0.072	3/8	5.2	Failure
C-23	3 3/4	0.145	0.072	3/8	5.2	Failure
C-24	3 5/8	0.145	0.072	3/8	5.2	Success
C-25	3 5/8	0.145	0.072	3/8	5.2	Success
C-26	3 3/4	0.145	0.072	3/8	5.2	Failure
C-27	3 3/4	0.145	0.072	3/8	5.2	Failure

Note: S is the split-hole spacing;
d' is the diameter of the Primacord;
d is the explosive charge diameter;
D is the split-hole diameter.

* Data which were ineffective.

the following two tests, tests C-26 and C-27. A successful split was not produced from these two tests. It is therefore concluded that the maximum successful spacing was 3 5/8 inches under the designed conditions.

b. Clay Filling.

1) Joint Filling Width $t=1/16$ Inch. Design of the test models was similar to that applied to the sand filling tests. Knowing that the maximum successful spacing for the 1/16 inch sand filling tests was 3 7/8 inches, a split-hole spacing of the same value was used in the design of test C-28 of the clay filling concrete test models. This test was a success, but as had happened on a previous sand filling test, the split line within the middle section of the test model was a small distance away from the center line of the model. For tests C-29 and C-30, the borehole spacing was increased to 4 inches. The results were not successful and no complete split was produced across the whole test block (see Figure D-13). The split-hole spacing was reduced back to 3 7/8 inches on the following test C-31 and a good split was created (see Figure D-14). The 3 7/8 inches spacing was again applied to tests C-32 and C-33. One of the two tests produced a split while the other resulted in a failure in which only minor fractures were formed along the center line of the model (see Table IV). Noticing that the concrete is not a perfect homogeneous material, a general conclusion is made that the maximum successful split-hole spacing was approximately 3 7/8 inches.

2) Joint Filling Width $t=1/8$ Inch. Test C-34 was made with split-hole spacing of $3 \frac{7}{8}$ inches. No split was created. A complete split was formed in test C-35 with the borehole spacing reduced to $3 \frac{3}{4}$ inches, although it was also noticed that the split line slightly deviated from the center line of the model and cratering from one borehole occurred (see Figure D-15). The split-hole spacing was then increased back to $3 \frac{7}{8}$ inches again and applied to test C-36. The result of this test was quite similar to that from test C-34 and no clear split fracture was found (see Figure D-16 and Table IV). However, when the split-hole spacing was reduced to $3 \frac{3}{4}$ inches in tests C-37 and C-38, no complete split line was achieved. Due to the shortage of prepared concrete, no further tests could be made to address the problem.

3) Joint Filling Width $t=1/4$ Inch. The splithole spacing used for test C-39 was 4 inches. No split was achieved (see Figure D-17). Tests C-40 and C-41 were carried out with a split-hole spacing of $3 \frac{5}{8}$ inches. No clear and continuous split across the test block was found in test C-41 while a good split was produced in test C-40 (see Figure D-18). For test C-42, the split-hole spacing was increased to $3 \frac{3}{4}$ inches. A continuous split was formed at the top of the test model, but not throughout the entire depth of the concrete block. It is considered reasonable to conclude that the maximum successful split-hole spacing is approximately $3 \frac{5}{8}$ inches.

TABLE IV
DATA OF CLAY-FILLED, TWO-JOINT CONCRETE MODEL TESTS

a. Clay Filling Width $t=1/16$ in.

Test No.	S(in.)	d'(in.)	d(in.)	D(in.)	D/d	Result
C-28	3 7/8	0.145	0.072	3/8	5.2	Success
C-29	4	0.145	0.072	3/8	5.2	Failure
C-30	4	0.145	0.072	3/8	5.2	Failure
C-31	3 7/8	0.145	0.072	3/8	5.2	Success
C-32	3 7/8	0.145	0.072	3/8	5.2	Failure
C-33	3 7/8	0.145	0.072	3/8	5.2	Success

b. Clay Filling Width $t=1/8$ in.

Test No.	S(in.)	d'(in.)	d(in.)	D(in.)	D/d	Result
C-34	3 7/8	0.145	0.072	3/8	5.2	Failure
C-35	3 3/4	0.145	0.072	3/8	5.2	Success
C-36	3 7/8	0.145	0.072	3/8	5.2	Failure
C-37	3 3/4	0.145	0.072	3/8	5.2	Failure
C-38	3 3/4	0.145	0.072	3/8	5.2	Failure

c. Clay Filling Width $t=1/4$ in.

Test No.	S(in.)	d'(in.)	d(in.)	D(in.)	D/d	Result
C-39	4	0.145	0.072	3/8	5.2	Failure
C-40	3 5/8	0.145	0.072	3/8	5.2	Failure
C-41	3 5/8	0.145	0.072	3/8	5.2	Success
C-42	3 3/4	0.145	0.072	3/8	5.2	Failure

Note: S is the split-hole spacing;
d' is the diameter of the Primacord;
d is the explosive charge diameter;
D is the split-hole diameter.

4. Effect of Discontinuity Filling Width. From the former two subsections it can be seen that the concrete model tests with sand or clay fillings were made with three different filling widths. For the fine siliceous sand filling and the clay filling, all the data on the filling width and the correspondent magnitude of the maximum successful split-hole spacing are listed in Table VI and VII.

For the cases in which clay was used as the filling material with discontinuity width of 1/16 inch the resulting data of the maximum successful spacing are only the rough conclusion from the model tests. Data of the maximum successful split-hole spacing, and the correspondent sand filling width are plotted in Figure 10. A linear correlation in the relationship between the sand filling width t and the maximum successful splithole spacing S_m can be tentatively represented by the following formula:

$$S_m = 5.33t^2 - 3t + 4.04$$

in which

S_m is the maximum successful splithole spacing, in.;

t is the discontinuity sand filling width, inch.

It should be noticed that there are two terms of t in this equation. One is linear in t and has a negative contribution to S_m while the quadratic term has a positive contribution.

TABLE V
 MAXIMUM SUCCESSFUL SPLIT-HOLE SPACING S_m
 AND CLOSED-DISCONTINUITY FREQUENCY n

n	S_m (in.)
0	4 1/2
1	4 *
2	3 7/8

* Equivalent data transformed the second mix concrete to the first mix concrete.

TABLE VI
 MAXIMUM SUCCESSFUL SPLIT-HOLE SPACING S_m
 AND SILICEOUS SAND FILLING WIDTH t

t (in.)	S_m (in.)
1/16	3 7/8
1/8	3 3/4
1/4	3 5/8

TABLE VII
 MAXIMUM SUCCESSFUL SPLIT-HOLE SPACING S_m
 AND CLAY FILLING WIDTH t

t (in.)	S_m (in.)
1/16	3 7/8
1/8	-----
1/4	3 5/8

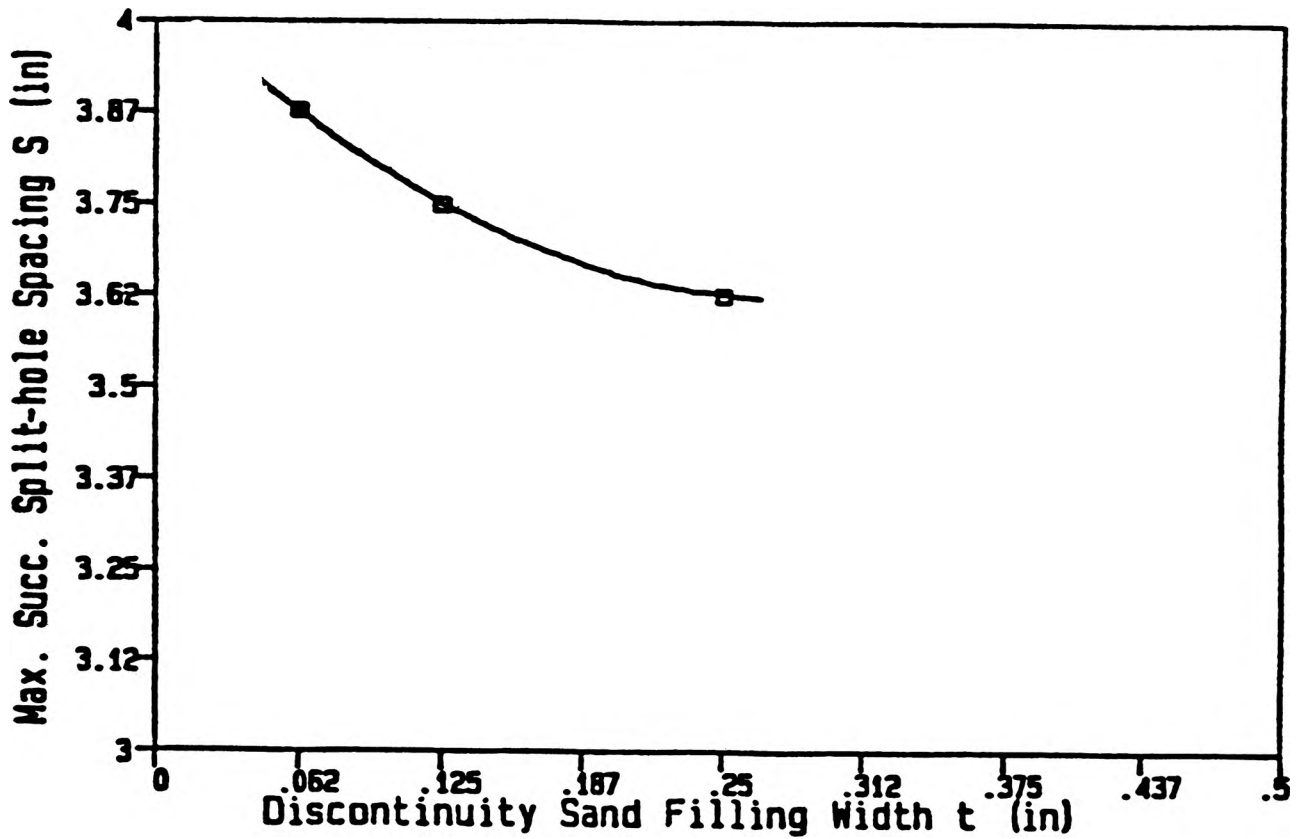


Figure 12: Maximum Successful Split-hole Spacing S_m
vs. Sand Filling Width t

Since the discontinuity width used in this experimental work is small and not more than 1/4 inch, the positive quadratic term cannot offset the negative linear one and the maximum split-hole spacing will be less than the constant 4.04(in.). On the other hand, from this equation, it seems that there are cases in which the maximum split-hole spacing can be greater than the constant term of 4.04 inches when the discontinuity width is about 9/16 inch or greater and the width of the layer between the two discontinuities approaches to zero.

Another interesting phenomenon occurred in both siliceous-sand-filled and clay-filled discontinuity model tests was the squeezing of the filling material (see Figures D-7, D-12, D-15, and D-17). The degree of the squeezing appeared to depend on the discontinuity filling width.

5. Effect of Discontinuity Plane Roughness. Three concrete model tests were made to observe the behavior of an uneven faced discontinuity. Each test model consisted of two concrete blocks of the second mix of concrete. Grooves 3/16 inch deep were made on the vertical interfaces of the two blocks by directly pouring the concrete mix into the grooved frames, so as to provide roughness to the discontinuities. The spacing of the grooves was 3/8 inches. In order to make the two concrete blocks completely contact at their interface, the discontinuity, grooves on one block coincided the humps on the other. Similar to other model tests discussed before, the discontinuity was also located midway between the split holes.

Test C-43 was made with a borehole spacing of $3 \frac{7}{8}$ inches. The splitting through the test model was incomplete. Fractures linking the split holes had been formed. For each half of the test model, fractures between the split holes were all connected to their nearest grooves at the discontinuity. Borehole spacing was then reduced to $3 \frac{3}{4}$ inches for the following two tests, tests C-44 and C-45. Both of the two tests resulted in a success splitting the model. The phenomena that split fractures from each borehole were extended to the groove's bottom of the discontinuity was again observed (see Figure D-20).

B. PLEXIGLAS MODEL TESTS

A split-hole spacing of 3 inches was chosen for all the Plexiglas model tests after preliminary tests. The dimension specifications for each test model were approximately the same, $9 \frac{1}{4}$ inches long, 6 inches wide, and 2 inches in thickness.

1. Continuous Model Test. The Plexiglas model for the first test consisted of a continuous Plexiglas block with no discontinuities. In the early stage of the event, each of the two boreholes appeared behaving independently, without mutual influence (see Figures E-3 and E-4) The stress waves from the two holes travelled outwards in a circle centered at their origins, the split hole. Following the stress wave front was the initiation of intense radial cracks from the borehole

periphery, behind which the explosion gases began to expand (see Table VIII, Figure 13, and Figures E-1 through E-8).

As the stress wave fronts from the two boreholes moved further outwards, they met midway between the boreholes and then, their interference occurred as they traveled further and overlapped each other. Both from the high speed camera pictures and the post-test examination of the test model, the fractures produced were all initiated at the borehole wall, no cracks being initiated midway between the split holes.

It took about 20 microseconds before the stress wave front reached the other borehole and several long fractures began to grow but, it was noticed, only along and around the line linking the two split holes (see Figures E-10, E-11 and E-12). The collision of the advancing stress wave with the borehole wall was likely the cause for the extension of the long fractures, remembering that the first portion of the advancing stress wave was a compressive stress pulse. Referring to mechanics theory, this compressive stress pulse will, at this point, cause a concentrated tangential tensile stress oriented perpendicular to the desired split line, and long fractures will be preferentially extended in this direction (see Figure E-23). At this point, the borehole side face, as well as the initiated radial cracks, will definitely be under the pressure from the rapidly expanding explosion gases which would also be an important factor for the extension of the long fractures.

Table VIII
DATA FOR CONTINUOUS PLEXIGLAS MODEL TEST

a. Dynamic Stress Wave Propagation Velocity v

Picture No.	D(mm)	d(mm)	T(us)	v(m/s)
E-2	19	32.8	7.5	----
E-3	30	51.7	10.0	3770
E-4	39	67.2	12.5	3086
E-5	47	81.0	15.0	2743
E-6	55	94.8	17.5	2743
E-7	62.5	107.8	20.0	2571
E-8	70	120.7	22.5	2571

b. Radial Cracking Propagation Velocity u

Picture No.	D(mm)	d(mm)	T(us)	v(m/s)
E-4	18	31.0	12.5	----
E-5	22	37.9	15.0	1370
E-6	24.5	42.2	17.5	857
E-7	26	44.8	20.0	514
E-8	27	46.6	22.5	343

Note: D is the diameter of the stress wave front measured on the photographs;
d is the actual diameter of the stress wave front;
D' is the diameter of the radial cracking circle measured on the photographs;
d' is the actual diameter of the radial cracking circle;
T is the time at which the picture was taken by the high speed framing camera.

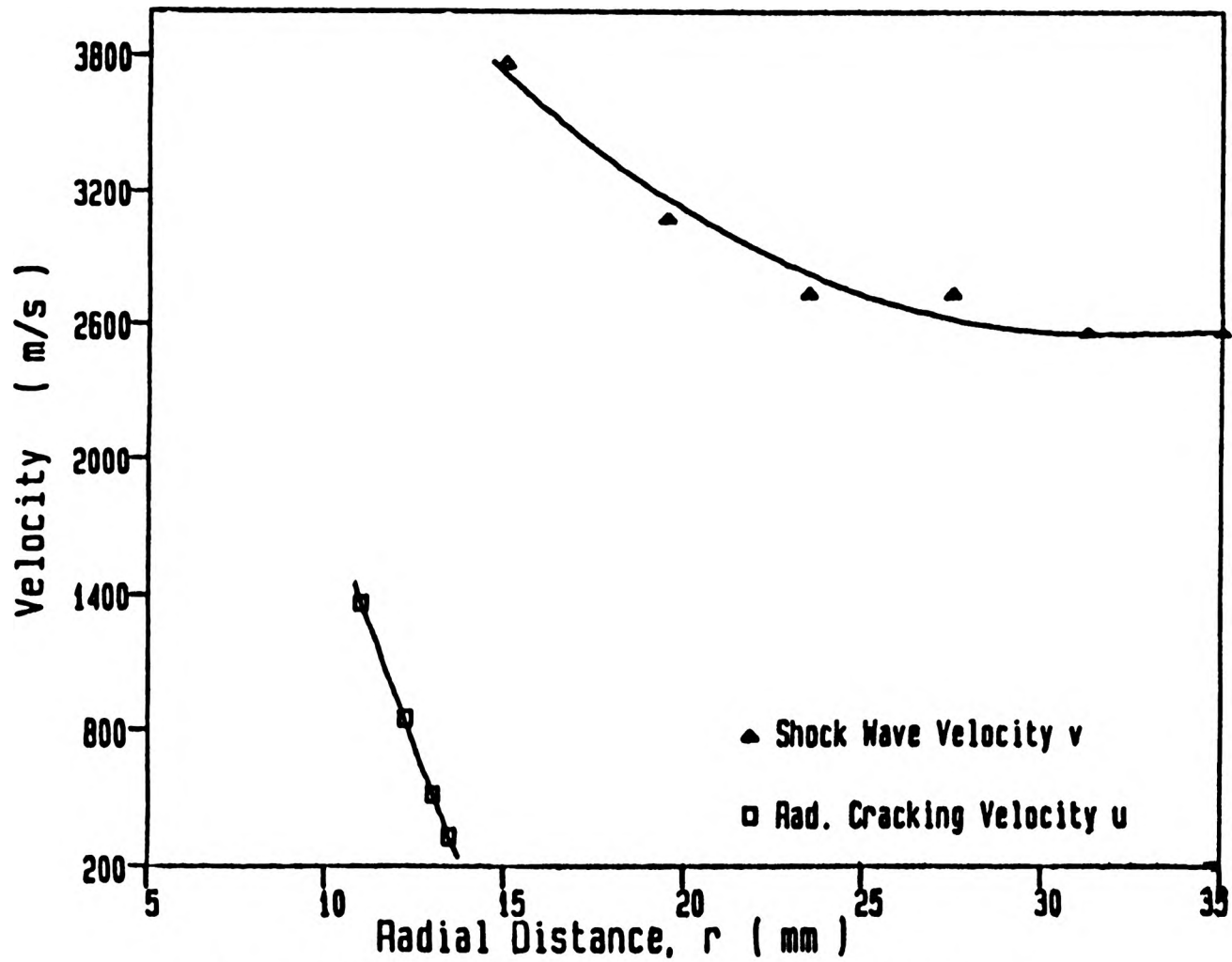


Figure 13: Shock Wave Propagation Velocity v
and Radial Cracking Velocity u
vs. Radial Distance r

The other information provided in the pictures taken by the high speed framing camera is the stress wave propagation velocity and the velocity of the radial crack extension. The interframe rate was 2.5 microseconds per frame for the pictures. The scale factor of the picture to the original test model was measured to approximately 0.58, seeing that the 3-inch borehole spacing in the original test model was about 1.75 inches in the picture. From Figures E-2 and E-3, it was found that the distance which the stress wave front moved was 5.5 mm, thus the stress wave front propagation velocity was found to be approximately 3770 meters per second. In the same way, the radial cracking velocity was found to be 1371 meters per second, seeing that the difference in the radial crack's lengths shown on the Figures E-4 and E-5 was about 2 mm.

2. Sand Filling Model Tests. These tests consisted of Plexiglas model test blasts with two sand filled discontinuities. The discontinuity widths for the test models were 1/16, 1/8, and 1/4 inches.

The radial cracking phenomena occurred during the early stages of the blasting event for each of the three model tests as happened in the continuous Plexiglas model test, (see Figures E-14, E-16 and E-18). Radial cracks were initiated at the borehole wall by the stress wave front before it passed away and the explosion gases began to expand. It appeared that the shock wave initiated radial cracks were extended by the expanding explosion gases.

As the stress wave front reached the discontinuity the propagation of the stress wave became a more complex process, while at the same time the explosion gases was interacting with the borehole wall and the radial cracks. When the discontinuity width was 1/16 inch in this Plexiglas model test, test No. 2, reflection of the wave from the discontinuities was not visible while the transmitted portions of the wave fronts were quite clear as they were interfering within the middle section of the test model (see Figure E-14). Minor cratering from the split hole to the discontinuities occurred at the late part of the process when the stress waves had already passed away and the explosion gases were still expanding within the split holes.

From Figure E-13, it can be seen that two long fractures were produced from one hole toward the end side of the model during the early stage of the event before other long radial cracks were created. It seems that these two long radial fractures were induced only by the dynamic stress pulses coming from the other hole but were not related to the explosion gas pressure. As the stress wave front moved further, the explosion gases expanded and a number of long radial cracks were initiated from the intensely radial cracked area and extended outward, (see Figures E-13, E-16, and E-18).

When the discontinuity width was increased to 1/8 inch in the Plexiglas test, test No. 3, the disturbance to the stress

wave propagation and the cratering effect, i.e., the serious fracturing specifically from the borehole towards the nearby discontinuities, were, to a certain degree, more obvious and severe than that when the discontinuity width was 1/16 inch in test No. 4. Moderate reflected stress waves from the discontinuities were found and shown in Figures E-16 as an example. Following this observation were the transmitted stress waves over the discontinuities and their interfering within the middle section of the test model (see Figures E-14, 16, and 18). Although a decrease in the intensity of the transmitted stress waves could not be calculated, the reduction of the distinctness of the fringe associated with the transmitted stress wave front implies that the stress waves had been attenuated through the discontinuity. From the point view of energy conservation, this seems reasonable since part of the energy present in the incident stress waves has been transformed into the reflected stress waves.

Cratering initiated during the late stage of the event when the stress waves had already disappeared and only the explosion gases were in action (see Figure E-24). Comparing the result to that from the previous test, it can be found that the cratering that occurred in this test was more severe. Squeezing of the filling material was also found in this test which is similar to that which occurred to some of the concrete model tests when the filling width was 1/8 and/or 1/4 inch.

For the test with a discontinuity filling width of 1/4 inch, only part of the gas expansion phase was recorded by the high speed framing camera and all the stress wave propagation process within the test model was missed due to a synchronization problem.

By examining the test model after the experiment and comparing it with the previous two tests, it can be seen that the cratering in this test was the most severe (see Figure E-22).

3. Closed Discontinuity Model Test. During the early stage of the event before the stress waves reached the closed discontinuities in this test, test No. 5, radial cracks were initiated in the same manner as in the previous tests. As the stress waves traveled outward from the boreholes to the discontinuities, no clear reflection was observed, and stress wave transmission over the discontinuities was easily visible (see Figures E-19 and E-20). From Figures E-19 and E-20 the distance from the transmitted stress wave front to the borehole center was about 22.5 mm which was 2 mm shorter than that for the stress wave front beyond the discontinuity. Thus it is shown that the propagation of the stress wave front over the discontinuity was delayed for about 8% of the radial distance, at the point about 13 microseconds after firing. Attenuation of stress waves through the closed discontinuity was similar to, but less severe than that for the 1/8 inch sand filled discontinuity model test.

V. CONCLUSIONS

When an explosive is detonated in a blasthole, a dynamic shock wave is generated and propagates outward with a velocity higher than the ultrasonic longitudinal velocity for the material. This shock wave is compressive in the radial direction of the borehole and causes a tangential tensile stress and thus initiates radial cracks around the borehole periphery. Following the dynamic stress wave propagation and the radial crack initiation is the rapid expansion of the high temperature explosion gases produced from the detonation of the explosive which fills and pressurize the borehole and subsequently penetrates into the radial cracks and largely contribute to their extension. In this process, the collision of the incident dynamic stress wave front from the neighboring borehole on the borehole boundary appears to be an important factor in the preferential propagation of the cracks in the direction of the axis between the two boreholes.

The results of the experimental investigation indicated that the presence of the discontinuities between split holes reduces both the maximum successful split-hole spacing and the regularity of the split profile. Radial cracking tends to preferentially develop towards but, stop at, the nearby discontinuities. Both discontinuity frequency and filling width reduce the maximum successful spacing to a limited

degree, except at their extremities. No obvious difference in the effects of siliceous sand filling and clay filling were found. The results of the tests using rough discontinuities revealed that the split fractures were preferentially extended to the nearest point of the nearby discontinuities, which implies that the profile of discontinuities can affect the regularity of the split line.

Cratering from split holes to nearby discontinuities appeared to be a most important problem regarding the regularity of the split profile. The cratering effect is minimum for closed joints without filling. To reduce and/or eliminate this problem and optimize rock splitting practices in the presence of distinct discontinuities, split holes should be drilled evenly straddling the discontinuities.

The examination of high speed framing photographs taken from Plexiglas model splitting tests revealed that when a stress wave reaches a discontinuity it cannot be totally transmitted through the discontinuity but is both attenuated and retarded to some degree, depending on discontinuity width. At the same time, the stress wave will be partly reflected in tension. However, it appears more likely that the cratering phenomenon is predominantly caused by the quasi-static gas pressure, since it occurs at a late stage of the event, when the stress waves have already dissipated.

Additionally, examination of high speed framing photographs indicated that the dynamic stress wave

propagation velocity is higher near the split hole than the laboratory measured ultrasonic longitudinal velocity V_r of the material and then, as it disperses outward from the hole, it rapidly decreases and reaches approximately the level of the longitudinal ultrasonic velocity V_r (see Appendix A: III). The magnitude of the radial cracks' extension velocity is approximately equal to one third of the stress wave propagation velocity, which is in agreement with previous work (Jaeger and Cook, 1968).

VI. RECOMMENDATIONS

The experimental work of this study suggests that further studies related to this area are needed in order to more completely address the problem. As such, the following items are recommended:

(1) Some kinds of rock, as encountered in field rock splitting practices, should be used in preparing test models.

(2) A wider range of discontinuity frequency should be used between split holes in order to further examine the effect of the discontinuity frequency on the maximum successful split-hole spacing and the regularity of the split face.

(3) Other filling materials, such as earth, water, a mixture of the two, a mixture of clay and siliceous sand, should be used in reduced-scale tests to investigate their behavior during the split blasting event.

(4) A more practical explosive loading method should be selected such that the reduced-scale tests can simulate field practice more closely. Boreholes may not be drilled all through the test model. Collar stemming of the boreholes could be used.

(5) Splitting panels should be extended from 2 split holes upwards in number.

(6) Field practice, observation, examination, and field experiments are needed to verify the results obtained from model-scale tests and then, final conclusions quantitatively specifying the effects of geological discontinuities on rock splitting operations can be made that are valid and effective in improving the reliability and efficiency of field rock splitting practices.

BIBLIOGRAPHY

- Ash, R.L., 1973. "The Influence of Geological Discontinuities on Rock Blasting." Unpublished Ph.D. Dissertation. University of Minnesota, Minneapolis.
- Ash, R.L., 1984. Mining 307 Lecture Notes, University of Missouri-Rolla.
- Aso, K., 1966. "Phenomena Involved in Pre-splitting by Blasting." Unpublished Ph.D. Thesis, Stanford University.
- Atchison, T. C., 1961. "The Effects of Coupling on Explosive Performance." Colorado School of Mines, Quarterly Vol. 56, No. 1. pp.163-170.
- Bair, B. E., 1959. "Use of High Speed Camera in Blasting Studies." U.S. Bureau of Mines, R.I. 5584.
- Baker, D. B., Fournery, W. L., and Holloway, D. C., 1979. "Photoelastic Investigation of Flaw Initiated Cracks and Their Contribution to the Mechanics of Fragmentation." Proceedings, 20th Symp. on Rock Mech., Austin, Texas. pp.119-26.
- Bleakney, E. Everett et al., 1984. "The Effect of Fracture Propagation to Single Air or Gauge Filled Discontinuities." Unpublished Paper, UMR, Rolla, Missouri.

- Britton, R. R. Konya, C. J., and Skidmore, D. R., 1980.
"Primary Mechanism for Breaking Rock with Explosives."
Proceedings, th Symp. on Rock. Mech. pp.942-49.
- Clark, G. B., 1966. "Blasting and Dynamic Rock Mechanics."
Proceedings, 8th Symp. on Rock Mech. Univ. of Min-
nesota. pp.463-499.
- Drake, A. A., Jr., 1952. "A Study of the Effect of Join-
ting on the Blasting of Granite." Unpublished M.S.
Thesis, University of Missouri-Rolla.
- Dupont, E. I., 1977. "Blasters' Handbook." Dupont de
Nemours and Company, Inc., 175th Anniversary Ed.,
Chapter 22.
- Duvall, Wilbur I. and Thomas C. Atchison, 1957. "Rock
Breakage by Explosives." U. S. BuMines, RI 5356.
- Field, J. E. and A. Ladegaard-Pedersen, 1971. "The Infl-
uence of the Reflected Stress Wave in Rock Blasting."
International Journal of Rock Mech. and-Min. Science,
Vol. 8, pp.213-226.
- Fourney, W. L., P. B. Baker and D. C. Holloway, 1983.
"Fragmentation in Jointed Rock Material." Proc.,
First Symp. on Rock Fragmentation by Blasting,
Lulea, Sweden. pp.505-32.
- Gates, M., 1964. "Blasting Design Criteria." Civil En-
gineering, Vol. 34, No. 1. pp. 54-55.

- Grant, C. H., 1965. "Design of Open Pit Blasts." Proc. of the 7th Symp. on Rock Mech., Penn. State Univ.
- Griffin, G. L., 1973. "Mathematical Theory to Pre-splitting Blasting." Proceedings, 11th Engineering Geology and Soils Engineering Symposium, Pocatello, Idaho.
- Haas, C. J., 1963. "On Fractures Produced in the Neiborhood of Openings by Impulsive Loads." M.S. Thesis, Colorado School of Mines.
- Hansen, P. G., 1985. Engineering Mechanics, 342 II, Lecture Notes. University of Missouri-Rolla.
- Hino, Kumao, 1965. "Fragmentation of Rock Through Blasting and Shock Wave Theory of Blasting." The 1st Annual Symp. on Rock Mech. Vol.51, No. 3. p.191.
- Holloway, D. C., Baker, D. B., and Fourney, W. L., 1980. "Dynamic Crack Propagation in Rock Plates." Proceedings, 21st U.S. Symp. on Rock Mech. Rolla, MO. pp.371-78.
- Jaeger J. C. and Cook, N. G. W., 1968. "Fundamentals of Rock Mechanics." London: Methuen Inc. pp.329-30.
- Johansson, C. H., and Persson, P. A., 1970. "Detonics of High Explosives." London: Academic Press. pp.263-67.
- Johnson, J. B., 1962. "Feasibility of Model Studies in Blasting Research." Proceedings, 5th Symp. on Rock Mech. Univ. of Minnesota, Minneapolis. pp.263-71.

Konya, C. J., Britton, R., and Lukovic, S., 1984.

"Removing some of the Mystery from Presplit Blasting." The Journal of Explosives Engineering. pp.20-22.

Konya, C. J., Barrett, D. and Ed Smith, 1986. "Pre-splitting Granite Using Pyrodex, A Propellant." 12th Annual Conference on Explosives and Blasting Tech., Society of Explosive Engineers. pp.

Kutter, H. K., and Fairhurst, C., 1967. "The Roles of Stress Wave and Gas Pressure in Pre-splitting." Proc. of the 9th Symp. of Practical Rock Mech. pp.265-84.

Kutter, H. K., 1967. "The Interaction Between Stress Wave and Gas Pressure in the Fracture Process of an Underground Explosion in Rock with Particular Application to Presplitting." Unpublished Ph.D. Dissertation, Univ. of Minnesota, Minneapolis.

Kutter, H. K. and Fairhurst, C., 1971. "On the Fracture Process in Blasting." International Journal of Rock Mechanics and Mining Science, Vol. 8, No. 3. pp.181-202.

Langefors, U. and B. Kihlstrom, 1963. "The Modern Techniques of Rock Blasting." New York: John Wiley and Sons. pp.296-320.

McCormick, J., 1972. "Geology and Blasting." Proceedings, 1st Conference on Drilling and Blasting, Phoenix, AZ.

- McKown, F. A., 1984. "Some Aspects of Design and Evaluation of Perimeter Control Blasting in Fractured and Weathered Proceedings, 10th Symp. on Rock Mech. and Blasting Tech. Lake Buena Vista, Florida. pp.120-139.
- Mellor, M., 1976. "Controlled Perimeter Blasting in Cold Regions." Proceedings, 2nd Conference on Explosives and Blasting Technique. Louisville, Kentucky. pp.280, 282-83.
- Nicholls, H. R., and Duvall, W. I. 1966. "Presplitting Rock in the Presence of A Static Stress Field." U.S. Bureau of Mines, RI 6808.
- Paine, S. R., D. K. Holmes, and E. Clark, 1961. "Pre-split Blasting at the Niagra Power Project." Explosives Engineer, Vol. 39, No. 3. pp.71-93.
- Porter, D. D. and C. Fairhurst, 1970. "A Study of Cracks Propagation Produced by the Sustained Borehole Pressure in Blasting." Proceedings, 12th Symp. on Rock Mech. pp.497-516.
- Raton, S. and Dhar, B. B., 1976. "Controlled Blasting in Rock Excavation Projects---A Review." Mining Magazine. pp.26-32.
- Rinehart, J. S., 1960. "On Fractures Caused by Explosions and Impacts." Colorado School of Mines, Quarterly, Vol. 55, No. 4. pp.17-48.

- Simha, K. R. Y., Holloway, D. C., and Fourney, W. L., 1983. "Dynamic Photoelastic Studies on Delayed Pre-split Blasting." Proceedings, 1st Int. Symp. on Rock Fragmentation by Blasting. Lulea, Sweden. pp.97-99.
- Simha, K. R. Y., and Fourney, W. L., 1984. "Studies on Explosively Driven Cracks under Confining in-situ Stresses." Proceedings, 25th US. Symp. on Rock Mech. pp.993-40.
- Singh, D. P. and V. R. Sastry, 1984. "Rock Fragmentation by Blasting---Influence of Joint Filling Material." Unpublished Paper. India.
- Smith, A. K. and R. Barnett, 1965. "Theoretical Consideration and Practical Applications of Smooth Blasting." Proceedings, 7th U.S. Symp. on Rock Mech.. pp.
- Trudinger, J. P., 1973. "An Approach to the Practice of Pre-splitting in Anisotropic Rock Masses." Bulletin of the Association of Engineers and Geologists, Vol. 10, No. 3. pp.161-71.
- Tyler, J., February 1986. Personal Communications. University of Missouri-Rolla.
- Wild, _____, 1977. "Attenuation of Stress Waves Influenced By Cementing Material." _____

- Winzer, S. R. and A. B. Ritter, 1980. "The Role of Stress Waves and Discontinuities in Rock Fragmentation: A Study of Fragmentation in Large Limestone Blocks." Proceedings, 21st U. S. Symp. on Rock Mech. Univ. of Missouri-Rolla, Rolla, MO. pp.362-70.
- Winzer, S. R., Douglass A. Anderson, and A. B. Ritter, 1983. "Rock Fragmentation by Explosives." 1st Int. Symp. on Rock Frag. by Blasting. Lulea, Sweden. pp.225-29.
- Worsey, P. N., 1985. Mining 402 Lecture Notes. University of Missouri-Rolla.
- Worsey, P. N., 1981. "Geotechnical Factors Affecting the Application of Pre-split Blasting to Rock Slopes." Ph.D. Thesis, University of Newcastle Upon Tyne, England.
- Worsey, P. N., I. W. Farmer and G. D. Matheson, 1981. "The Mechanics of Pre-splitting in Discontinuous Rock." Proceedings, 22nd U.S. Symp. on Rock Mech., M.I.T. pp.205-10.
- Worsey, P. N., 1984. "The Effect of Discontinuity Orientation on the Success of Pre-split Blasting." Proc. 10th Annual Conference on Explosives and Blasting Technique. pp.197-205.

Worsey, P. N., and Qingshou Chen, 1986. "The Effect of Rock Strength on Perimeter Blasting and the 'Blasability of Massive Rock." 12th Annual SEE Conf. on Expl.&Blast Tech.-Mini Research Symp., Atlanta, GA.

VITA

Shijie Qu was born on April 7, 1956 in Hebei province of the People's Republic of China. He received his primary and secondary education in Caozhuang Primary School and Yangyuan Middle School. He attended the Department of Mining Engineering of Beijing University of Iron and Steel Technology in October 1978 and graduated with a Bachelor of Science degree in Mining Engineering in July 1982.

He has been enrolled in the Graduate School of the University of Missouri-Rolla since May 1984 and held a scholarship from Ministry of Education of People's Republic of China.

APPENDIX A

PROPERTIES OF CONCRETE AND PLEXIGLAS

TABLE A-I
PROPERTIES OF THE FIRST MIX OF CONCRETE

Mix Proportions, by Weight:

17% Water

17% Portland Cement

66% Fine Building Sand

Mechanical Properties:

Specific Gravity(dry)	2.15
Compressive Strength(dry)	765.0 psi
Tensile Strength(dry)	267.0 psi
Longitudinal Wave Velocity(dry)	12470 fps
Shear Wave Velocity(dry)	8840 fps

TABLE A-II
PROPERTIES OF THE SECOND MIX OF CONCRETE

Mix Proportions, by Weight:

17% Water

17% Portland Cement

66% Fine Building Sand

Mechanical Properties:

Specific Gravity(dry)	1.97
Compressive Strength(dry)	690.0 psi
Tensile Strength(dry)	235.0 psi
Longitudinal Wave Velocity(dry)	11780 fps
Shear Wave Velocity(dry)	8330 fps

TABLE A-III
PROPERTIES OF PLEXIGLAS

Physical Properties:

Specific Gravity: 1.19

Optically Transparent

Mechanical Properties:

*Compressive Strength	10000-12000 psi
*Tensile Strength	7000-8000 psi
Longitudinal Wave Velocity V_r	9070 fps
Shear Wave Velocity	4455 fps

* After Haas, C. J., 1963.

APPENDIX B

PHYSICAL PROPERTIES OF FILLING MATERIALS

Siliceous Sand:

Specific Gravity(wet): 1.59

Size: 100 mesh

Clay Filling:

Specific Gravity(wet) 1.56

Size: 250 mesh

APPENDIX C

WAVE TRAPS

Theory of Spalling

When a compressive stress pulse traveling through a body encounters a free face, it will be reflected as a tensile pulse which travels back into the body (Duvall and Atchison, 1965; Rinehart, 1960).

It is well known that the compressive strength of a solid material, such as rock, concrete, and Plexiglas, is several times higher than its tensile strength. Hence, although the material remains undamaged when a compressive pulse passes through it, a failure can still occur under the action of the tensile pulse. Fractures oriented parallel to the free faces can be induced as a result, assuming a normal incidence of the compressive pulse to the free face. This fracturing phenomenon is known as spalling.

Spalling in real materials is complicated by a number of factors such as attenuation, geometrical divergence, imperfect reflection, inhomogeneities of the material, and the time required to initiate fracture. However, so as to give a general description of the spalling process, these factors will be neglected and only an ideal situation will be discussed for convenience.

First, consider a material such as rock which is strong in compression but comparatively weak in tension to a certain degree. Second, consider a triangular-shape longitudinal compressive pulse whose peak value is much greater than that of the tensile strength of the rock. As the compressive pulse advances normally to the free face, it will begin to be reflected as a tensile pulse as shown in Figure C-1. The peak value of the reflected tensile pulse will be constantly changing and become the algebraic sum of the tension and compression at the point and time. As the incident compressive pulse approaches the free face, the peak value of the reflected tensile pulse will be increasing until it reaches the tensile strength c_t of the rock and finally results in failure of the rock as open fractures oriented parallel to the free face (see figure C-1).

Figure C-2 shows a multiple spalling process. There are several aspects to be studied for this multiple spalling process. First, after the first slab moves away from the body a tail of the compressive pulse can still remain in the body and keep traveling toward the newly created free face. If the peak value of the remaining compressive pulse is still greater than the tensile strength of the rock, a second slab can be created in the same manner, and so on. Second, when a free slab is formed, the part of the resultant tensile pulse which remains in between the old and the newly created free face is now trapped within the free slab, which clearly means a

reduction of the magnitude of the resultant pulse left in the body. Additionally, the peak value of the resultant tensile pulse will never exceed the tensile strength of the medium through which the pulses travel.

Theory of Wave Traps

As stated before in Chapter II, free faces are usually located so far from any free face that it can be considered there is no spalling effect for the rock splitting practices. However, as for this experimental work, concrete models and Plexiglas models of limited dimension are used to simulate field conditions. A reasonable possibility may then exist that the side faces of the model have an influence on the splitting process. Therefore, special attention has to be made to eliminate the free face influence and wave traps are needed.

Wave traps are virtually an extension of the test block (Worsey, 1981). The interface of the block and the wave trap functions as a continuous fracture plane which encloses the side faces of the block (see Figure C-3). The wave traps are attached to the test block with a nominal pressure which keeps them in contact.

As the incident compressive pulse from the charges approaches the interface between the wave trap and the test block, it further tightens the interface and transmits through it without being affected, providing that the wave

trap and the test block are of the same material and the interface is in a perfect condition. Otherwise, if the material of the wave traps has a higher impedance than that of the test model, a reflected compressive pulse will be induced, and vice versa. The level of the reflected compressive pulse or the reflected tensile pulse from the interface is dependent upon the impedances of the two materials. When the tensile pulse reflected from the outer side of the wave trap reaches the interface, it cannot be transmitted through but will be reflected back outwards from the interface which is in fact a continuous break. Thus the test block is protected from any reflected dynamic waves.

Wave Trap Design

There are two important factors which should be considered when designing a Wave trap (Worsey, 1981). First, as mentioned before, the pressure exerted on the test blocks by the wave trap should be kept to a minimum level so as to avoid a tectonic stress effect upon the splitting process. Second, the width of the wave trap must be equal to or greater than that of the incident compressive pulse. Otherwise, the incident stress pulse cannot be totally transmitted into the wave trap before it begins to reflect at the outside face of the wave trap. As a result, part of the incident stress pulse will be left within the test block and tensile reflection at the side surfaces can occur. However, if such a case may

occur, it will be fairly negligible in magnitude compared with the maximum value of the reflected tensile pulse when a wave trap is not used.

The wave trap designed consisted of plain plywood plates which were cut to a size consistent with the test blocks. Heavy metal pieces and bolts with spring and rubber washers were used to stabilize the plywood plates and the test blocks. The thickness of the plywood plates used was approximately one inch, which was considered much greater than the compressive wave length.

It was also noticed that the effectiveness of a wave trap is affected by the degree of impedance matching of the test model and the wave trap (here it was plywood) and by the interface touching conditions of the two materials. Obviously, the impedances of either concrete or Plexiglas and plywood were much different. The sawed side faces of the concrete models were not of the same smoothness as that of plywood. Since then, the wave traps were used for the purpose of helping alleviate the reflection effect, if any, while main effort was made in the dimensional design of the test models.

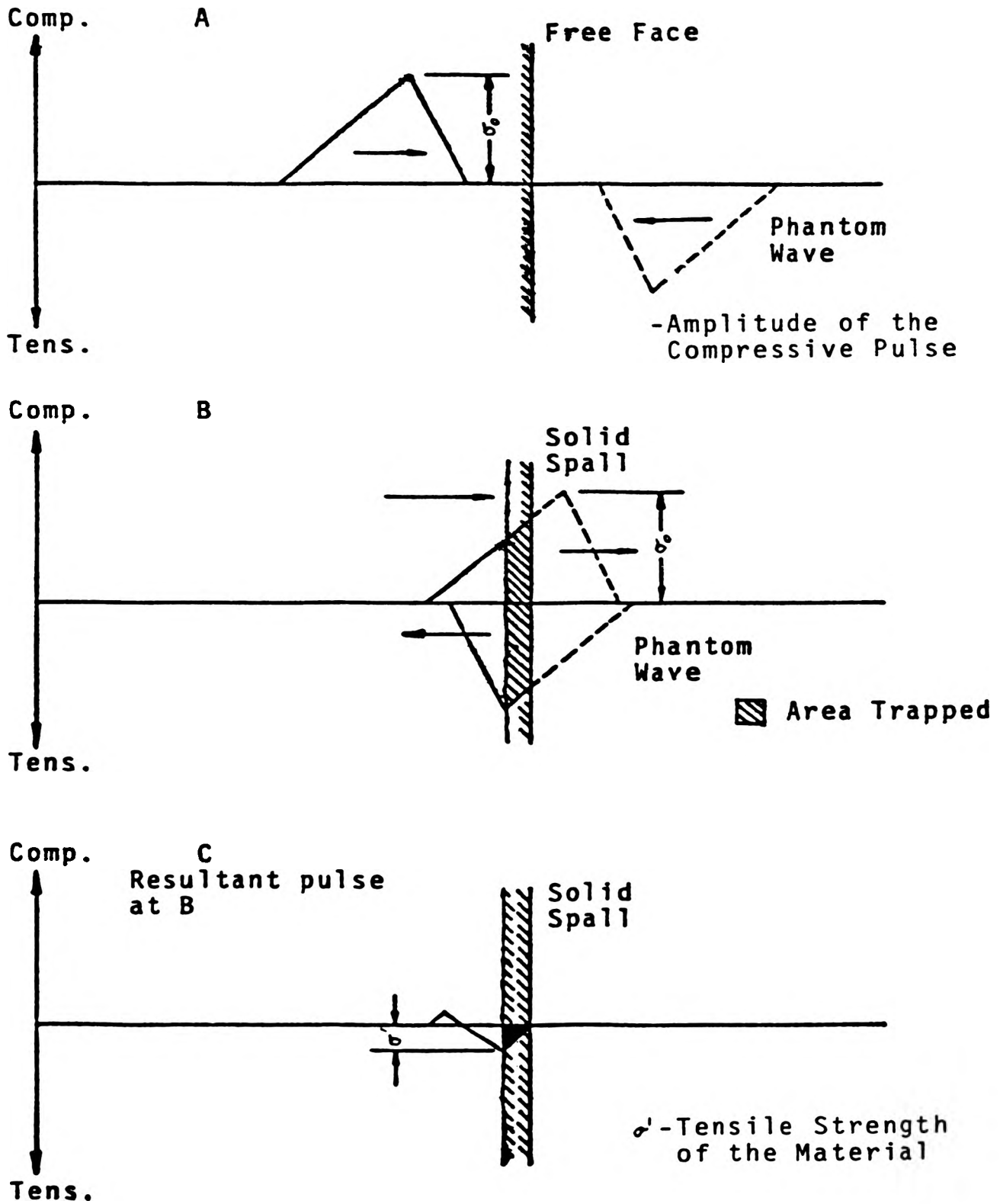


Figure C-1: Mechanics of Free Surface Spalling

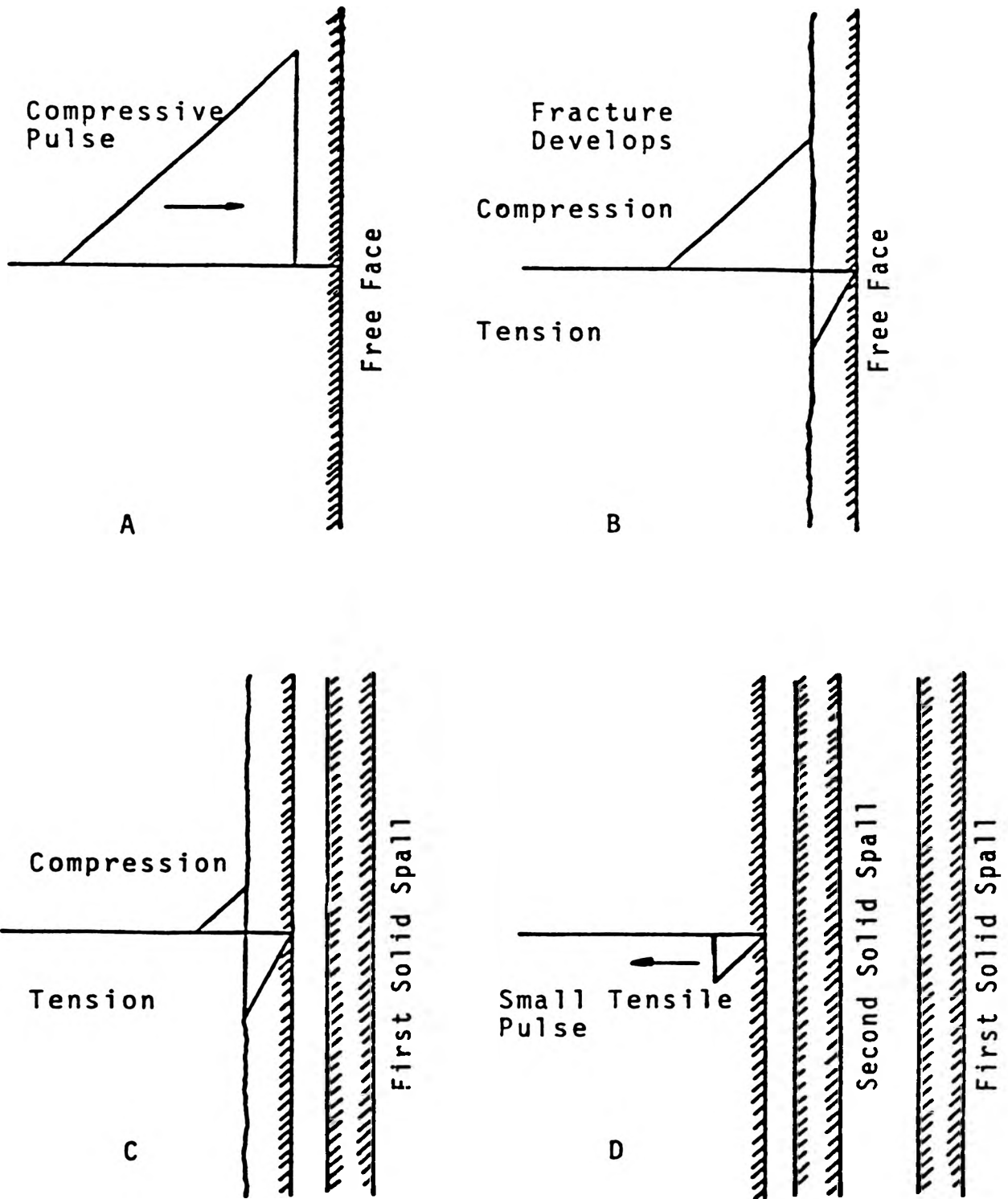


Figure C-2: Multiple Spalling of Free Surfaces
 (after Worsey, 1981)

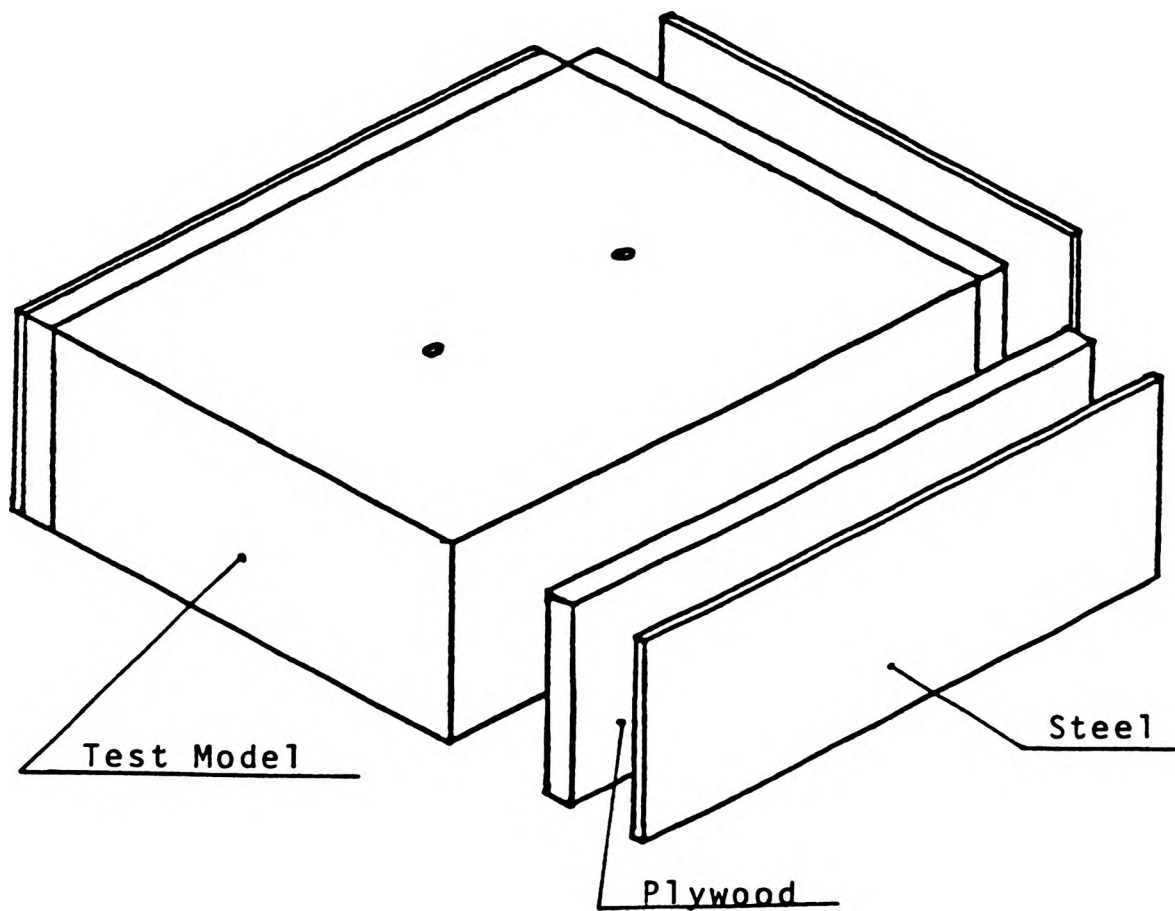


Figure C-3: Wave Trap Mechanics
(after Worsey, 1981)

APPENDIX D

DATA AND PHOTOGRAPHS OF CONCRETE MODEL TESTS

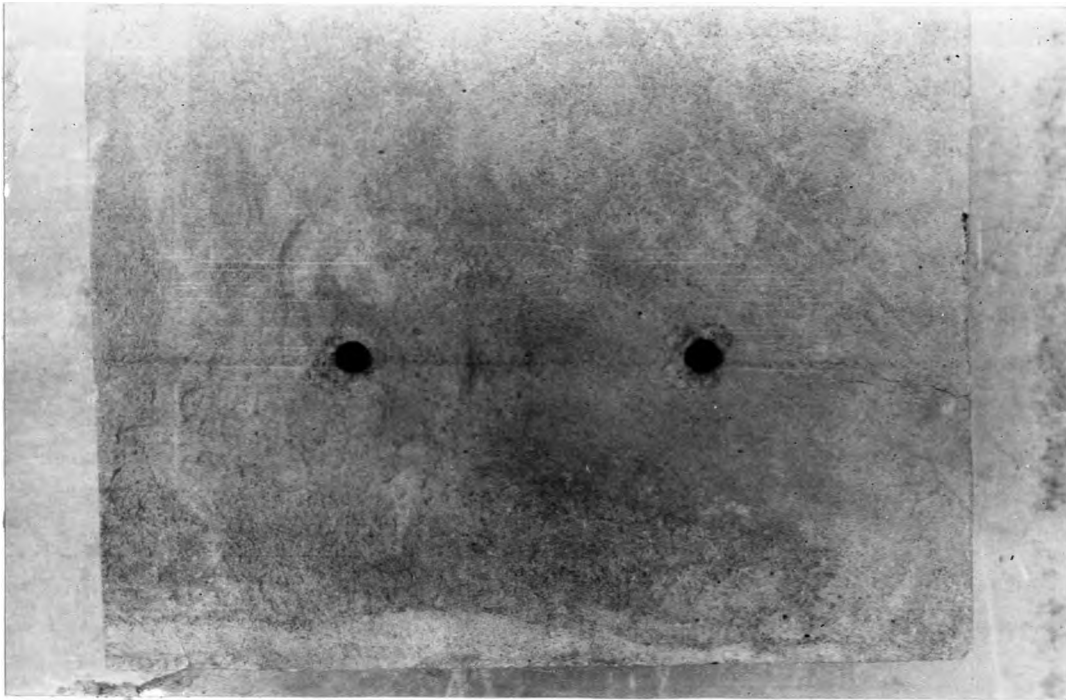


Figure D-1: Continuous Concrete Model Test:
Test C-1, S=5 in., A Failure

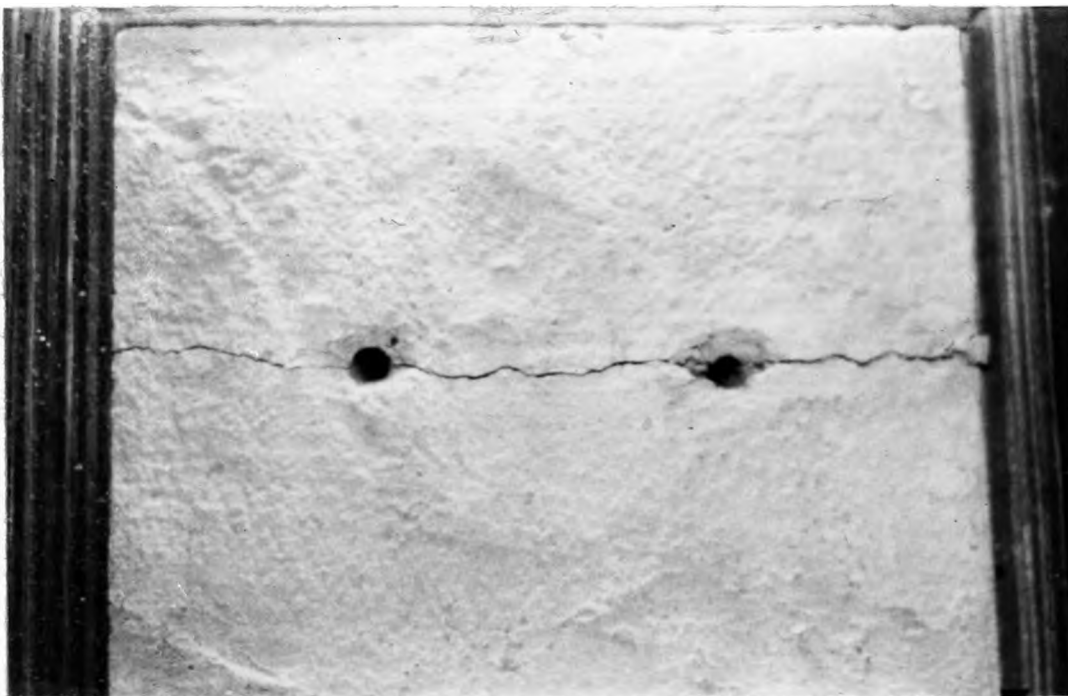


Figure D-2: Continuous Concrete Model Test:
Test C-3, S=4 1/2 in., A Success



Figure D-3: Single Closed Joint Concrete Model Test:
Test C-6, $S=4\frac{1}{2}$ in., A Success



Figure D-4: Single Closed Joint Concrete Model Test:
Test C-7, $S=5\frac{1}{4}$ in., A Failure

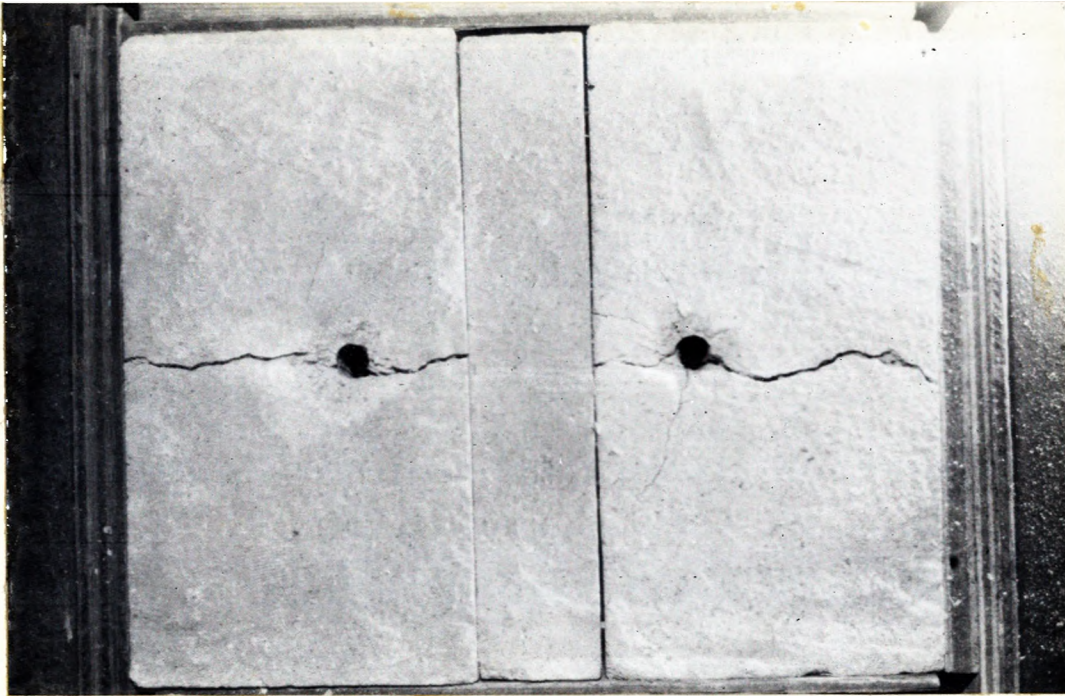


Figure D-5: Two Closed Joint Concrete Model Test:
Test C-13, S=4 in., A Failure



Figure D-6: Two Closed Joint Concrete Model Test:
Test C-12, S=3 7/8 in., A Success



Figure D-7: 1/16 in. Sand Filled, Two-Joint Concrete
Model test: Test C-15, S=4 in., A Failure



Figure D-8: 1/16 in. Sand Filled, Two-Joint Concrete
Model test: Test C-16, S=3 7/8 in., A Success



Figure D-9: 1/8 in. Sand Filled, Two-Joint Concrete
Model Test: Test C-21, $S=3 \frac{7}{8}$ in., A Failure.



Figure D-10: 1/8 in. Sand Filled, Two-Joint Concrete
Model Test: Test C-19, $S=3 \frac{3}{4}$ in.



Figure D-11: 1/4 in. Sand Filled, Two-Joint Concrete
Model Test: Test C-22, S=4 1/4 in., A Failure.



Figure D-12: 1/4 in. Sand Filled, Two-Joint Concrete
Model Test: Test C-24, S=3 5/8 in., A Success



Figure D-13: 1/16 in. Clay Filled, Two-Joint Concrete
Model Test: Test C-29, S=4 in., A Failure



Figure D-14: 1/16 in. Clay Filled, Two-Joint Concrete
Model Test: Test C-31, S=3 7/8 in., A Success



Figure D-15: 1/8 in. Clay Filled, Two-Joint Concrete
Model Test: Test C-35, S=3 3/4 in., A Success



Figure D-16: 1/8 in. Clay Filled, Two-Joint Concrete
Model Test: Test C-36, S=3 7/8 in., A Failure



Figure D-17: 1/4 in. Clay Filled, Two-Joint Concrete
Model Test: Test C-39, S=4 in., A Failure



Figure D-18: 1/4 in. Clay Filled, Two-Joint Concrete
Model Test: Test C-41, S=3 5/8 in., A Success



Figure D-19: Grooved Discontinuity Concrete Model
Test: Test C-43, $S=4 \frac{7}{8}$ in., A Failure.
Split Extended to the Grooves' Bottom

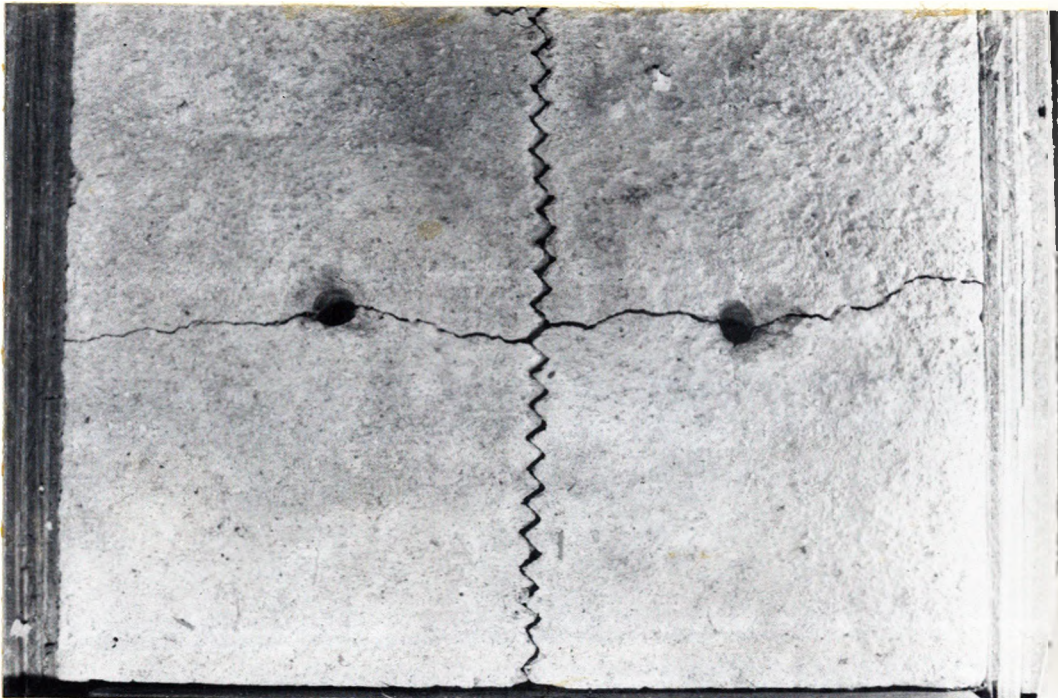


Figure D-20: Grooved Discontinuity Concrete Model
Test: Test C-44, $S=4 \frac{3}{4}$ in., A Success.
Split Extended to the Grooves' Bottom

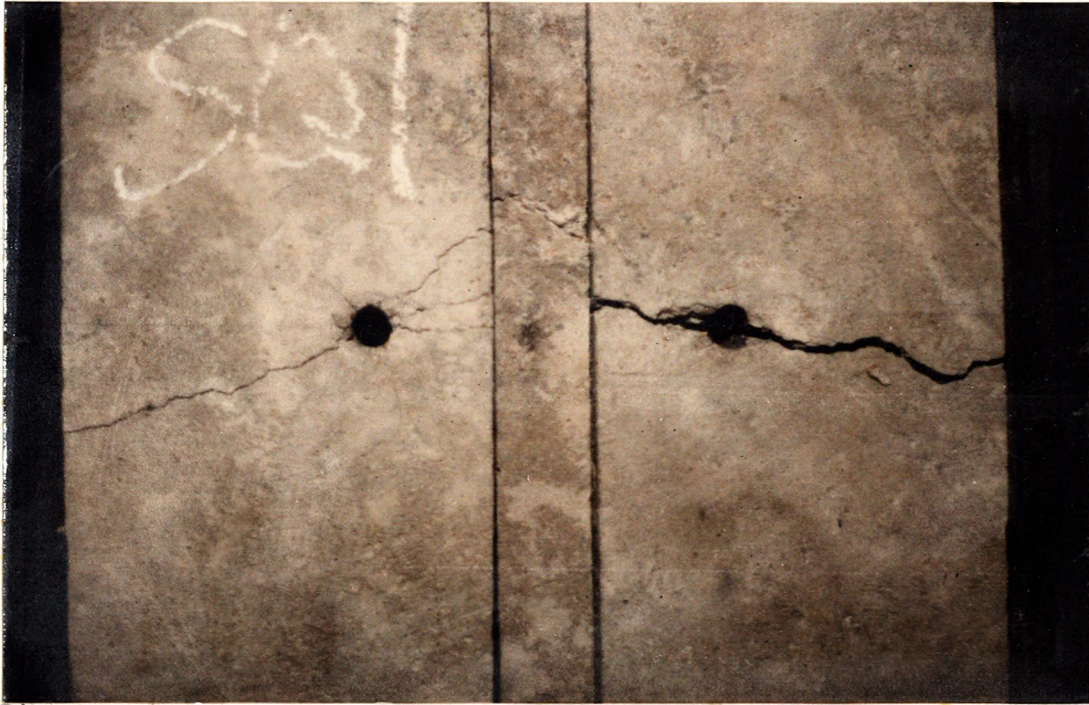


Figure D-21: Two-Closed-Joint Concrete Model Test:
Test C-9, $S=3\frac{3}{4}$ inch. Split within the
Middle Section Deviated from Centerline



Figure D-22: 1/8 in. Sand Filled, Two-Joint Concrete
Model Test: Test C-19, $S=3\frac{3}{4}$ inch, Cratering
Occurred from Boreholes to Discontinuities

APPENDIX E

DATA AND PHOTOGRAPHS OF PLEXIGLAS MODEL TESTS

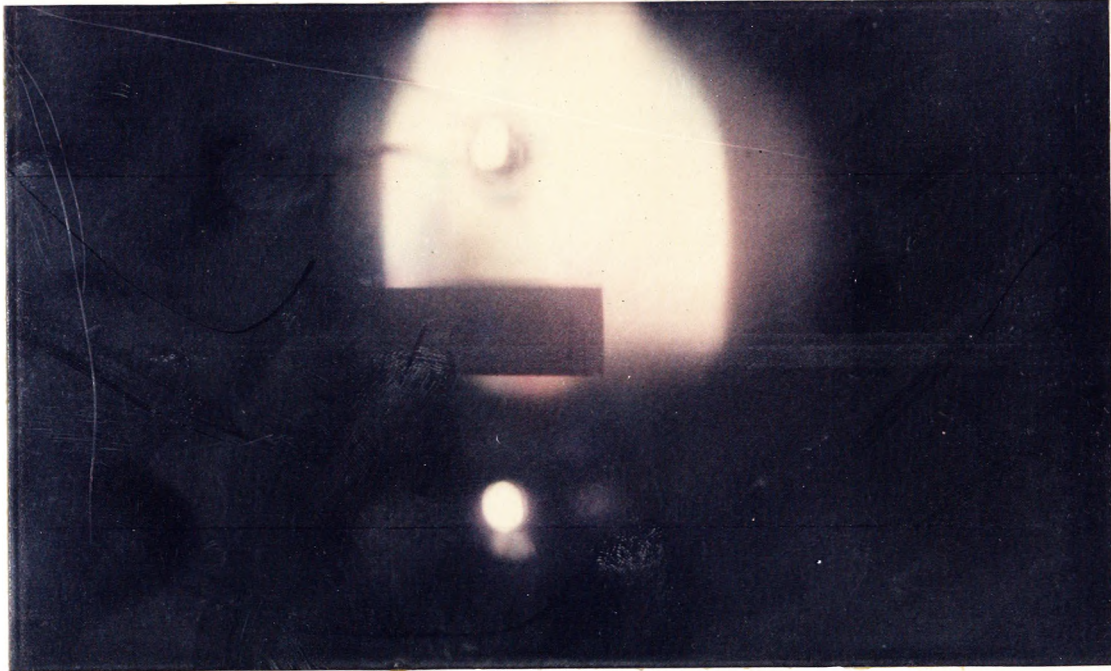


Figure E-1: Plexiglas Test No. 1: Continuous Plexiglas Model Test. 5.0 Microseconds after Firing

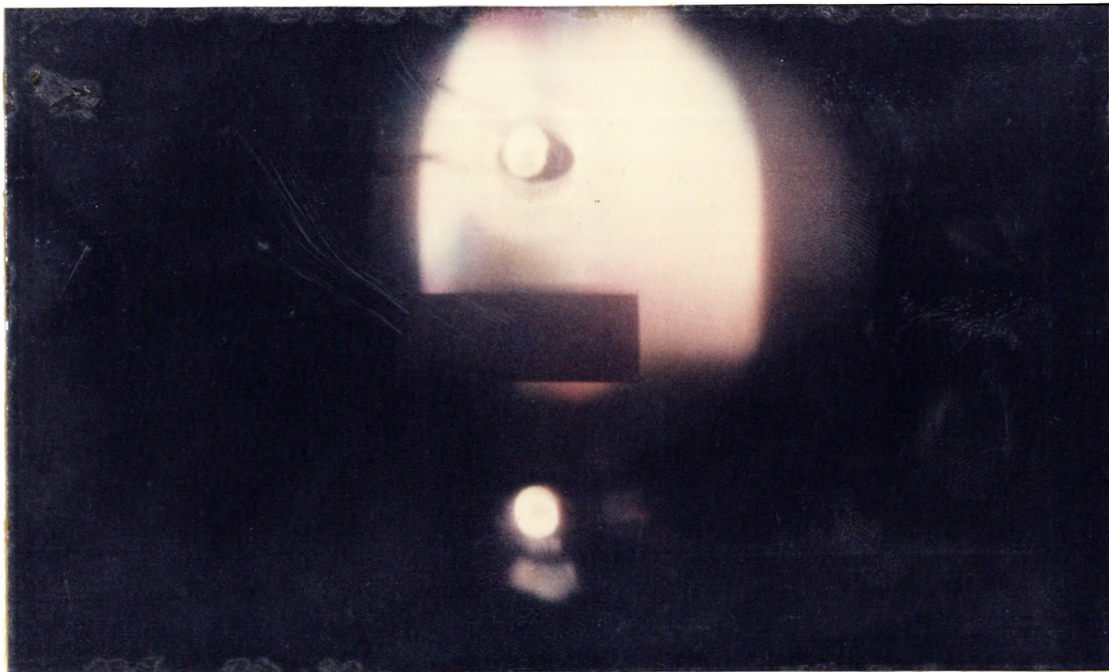


Figure E-2: Plexiglas Test No. 1: Continuous Plexiglas Model Test. 7.5 Microseconds after Firing

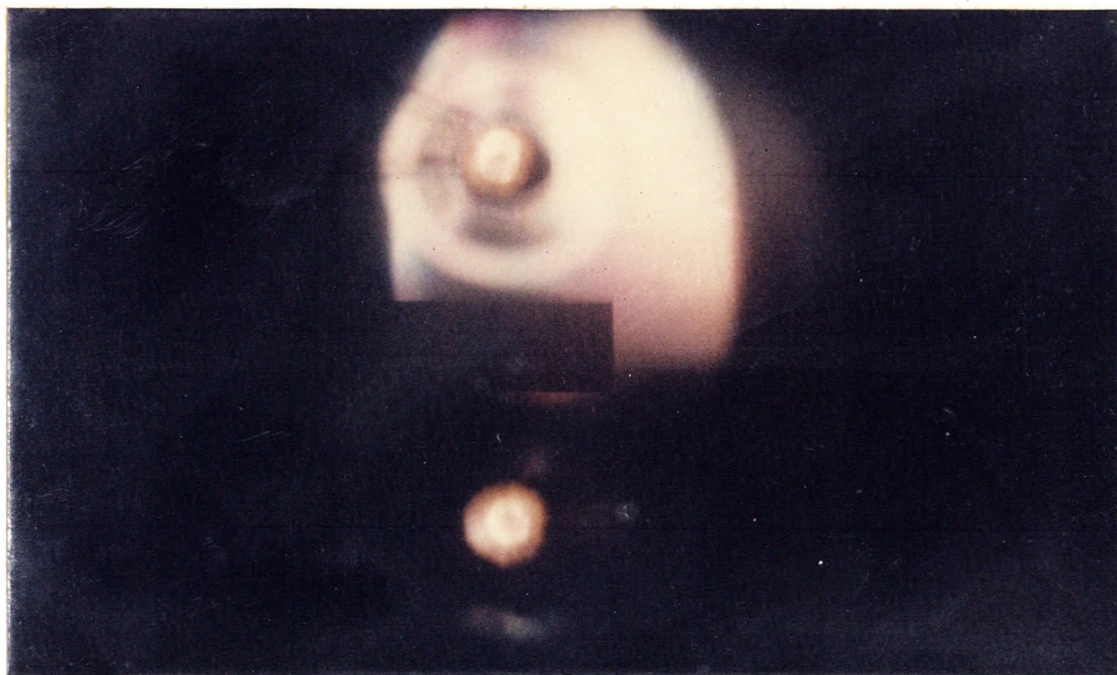


Figure E-3: Plexiglas Test No. 1: Continuous Plexiglas Model Test. 10.0 Microseconds after Firing

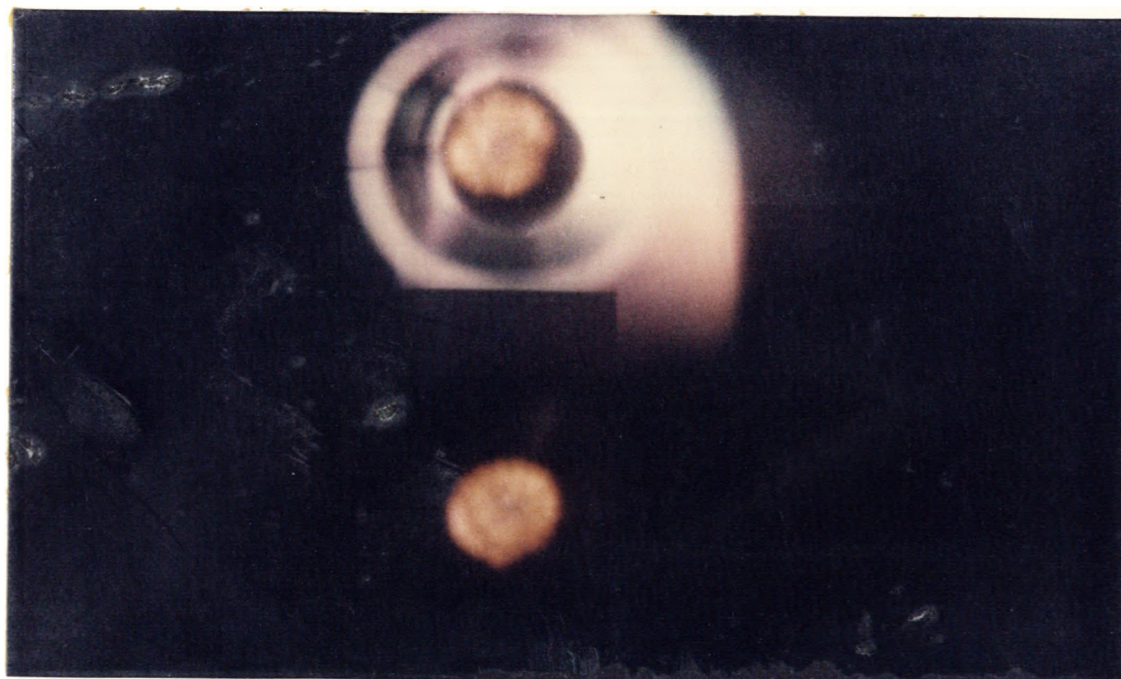


Figure E-4: Plexiglas Test No. 1: Continuous Plexiglas Model Test. 12.5 Microseconds after Firing

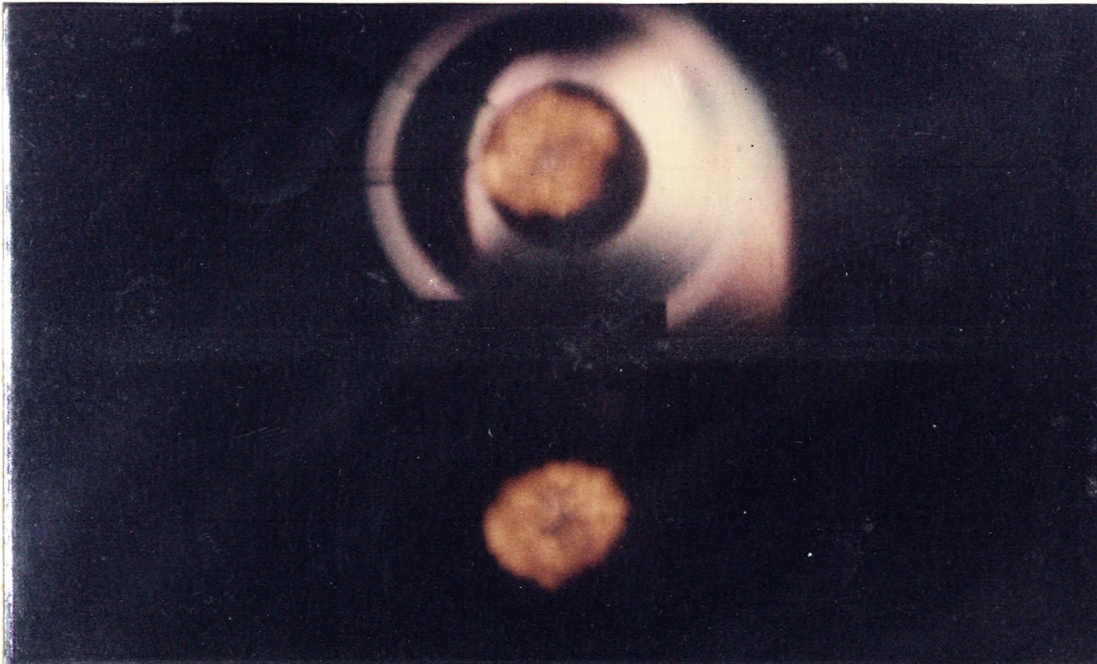


Figure E-5: Plexiglas Test No. 1: Continuous Plexiglas Model Test. 15.0 Microseconds after Firing

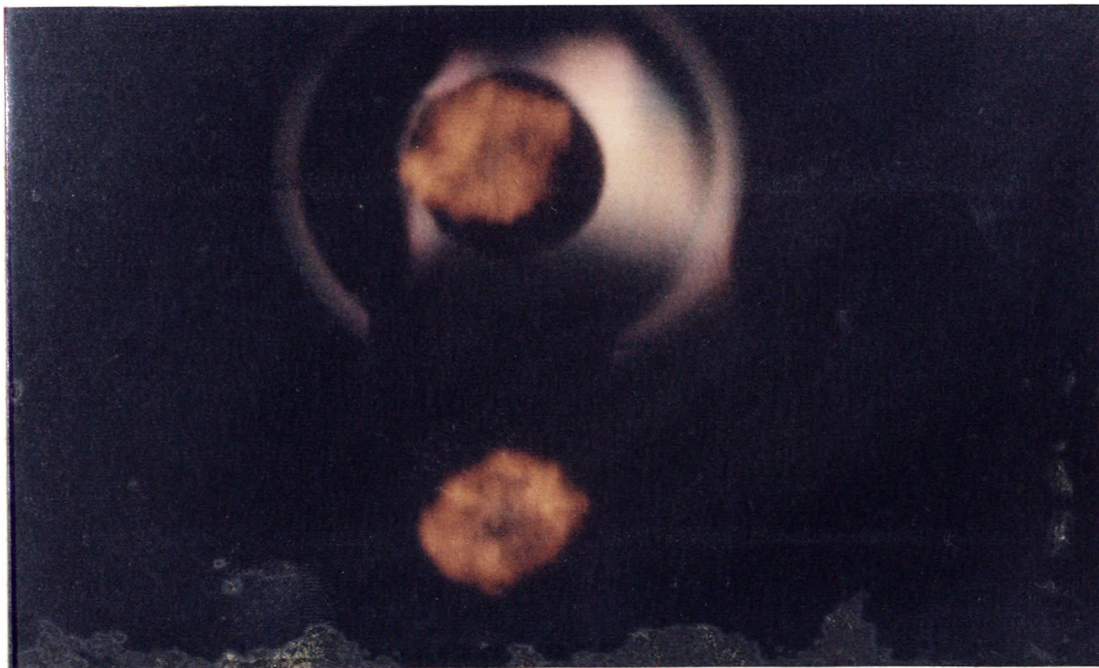


Figure E-6: Plexiglas Test No. 1: Continuous Plexiglas Model Test. 17.5 Microseconds after Firing

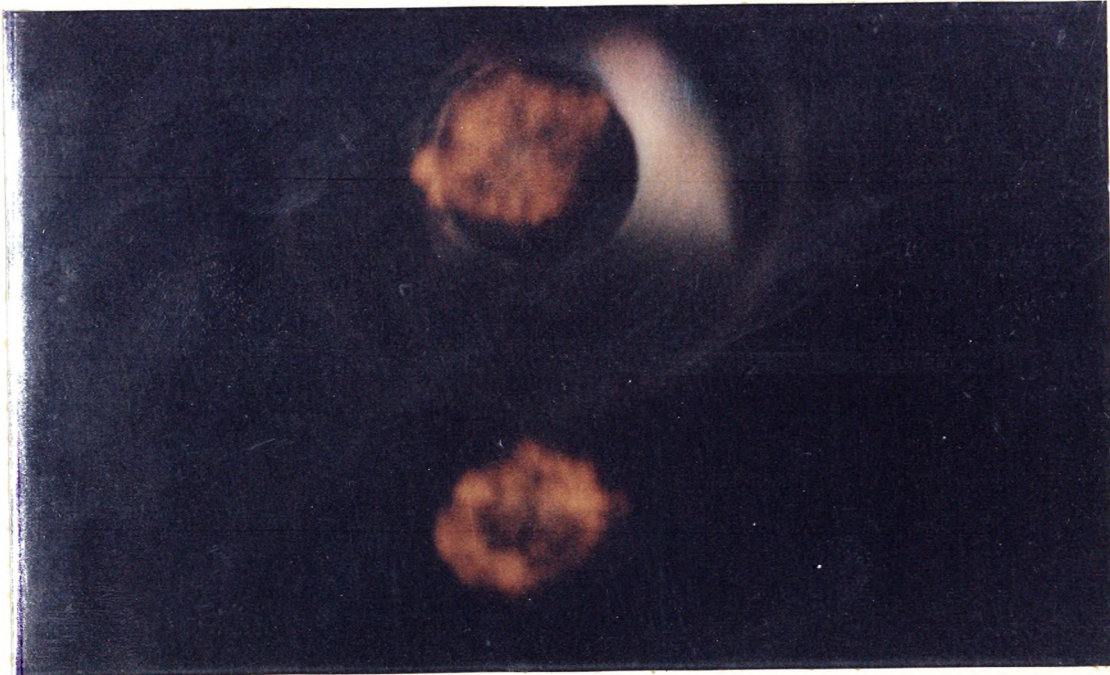


Figure E-7: Plexiglas Test No. 1: Continuous Plexiglas Model Test. 20.0 Microseconds after Firing

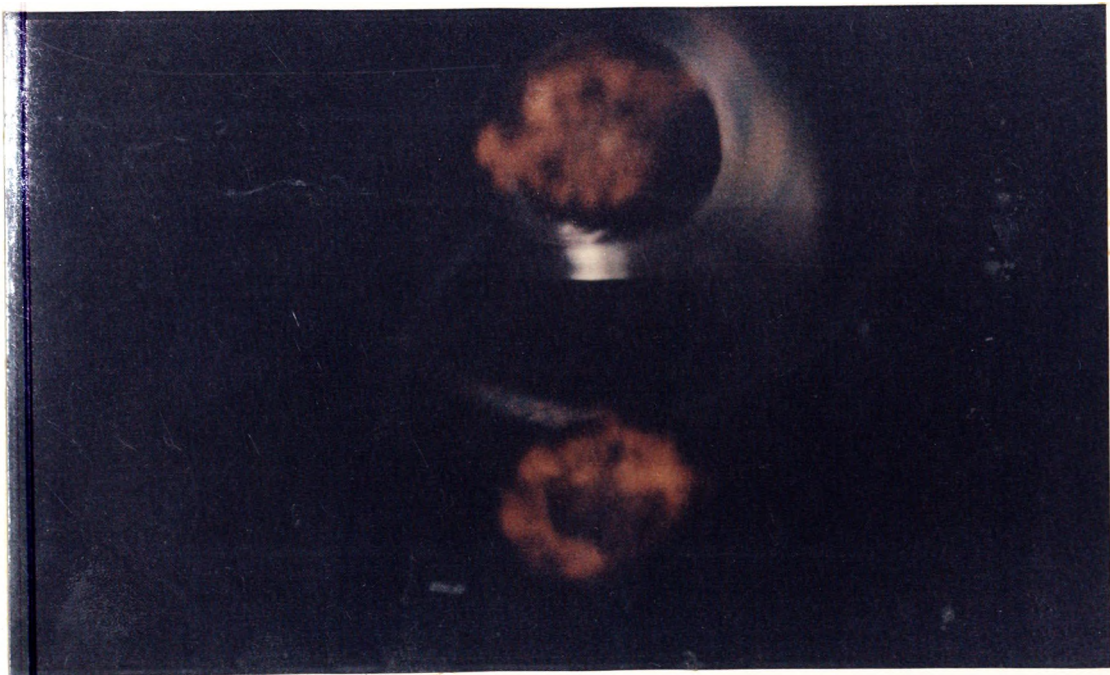


Figure E-8: Plexiglas Test No. 1: Continuous Plexiglas Model Test. 22.5 Microseconds after Firing

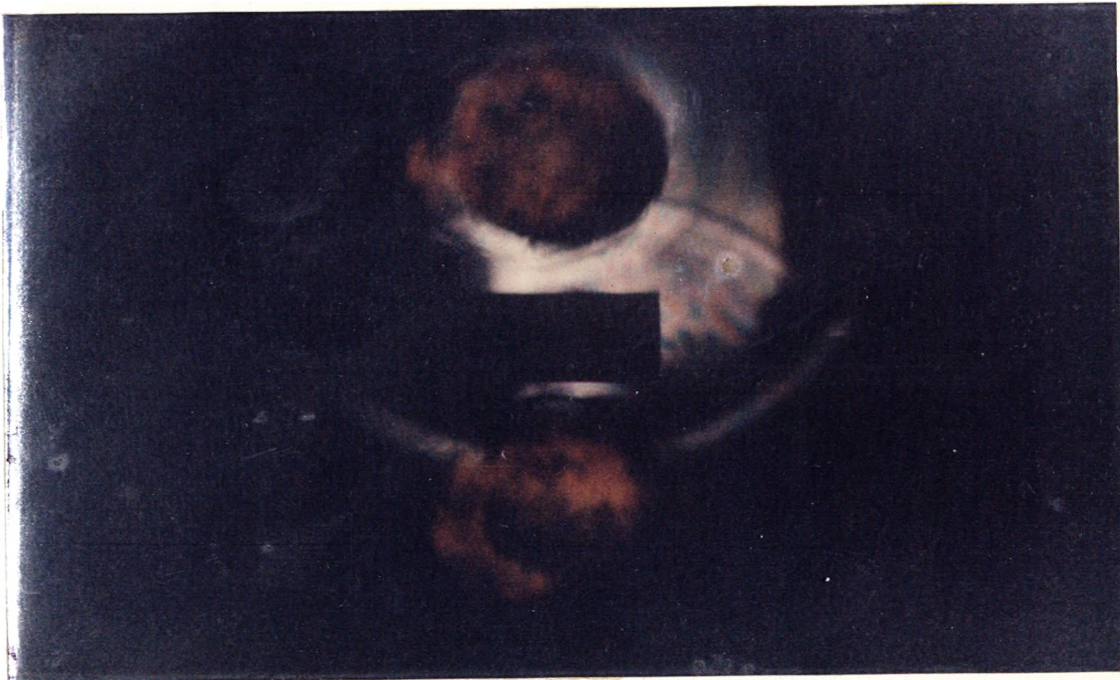


Figure E-9: Plexiglas Test No. 1: Continuous Plexiglas Model Test. 25.0 Microseconds after Firing

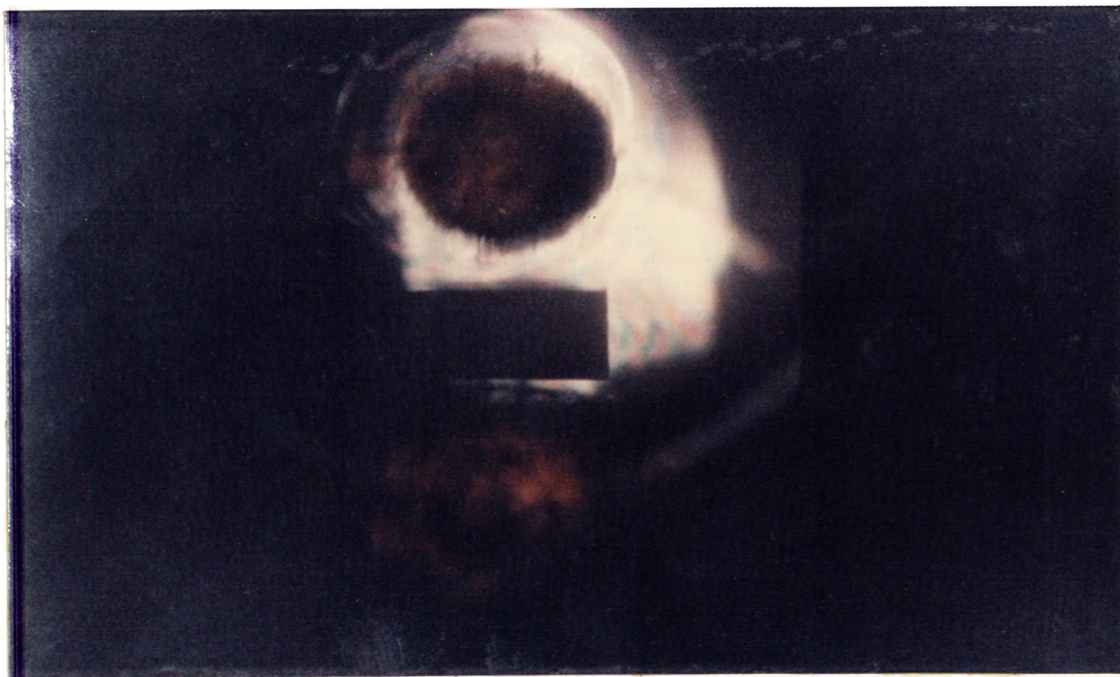


Figure E-10: Plexiglas Test No. 1: Continuous Plexiglas Model Test. 27.5 Microseconds after Firing

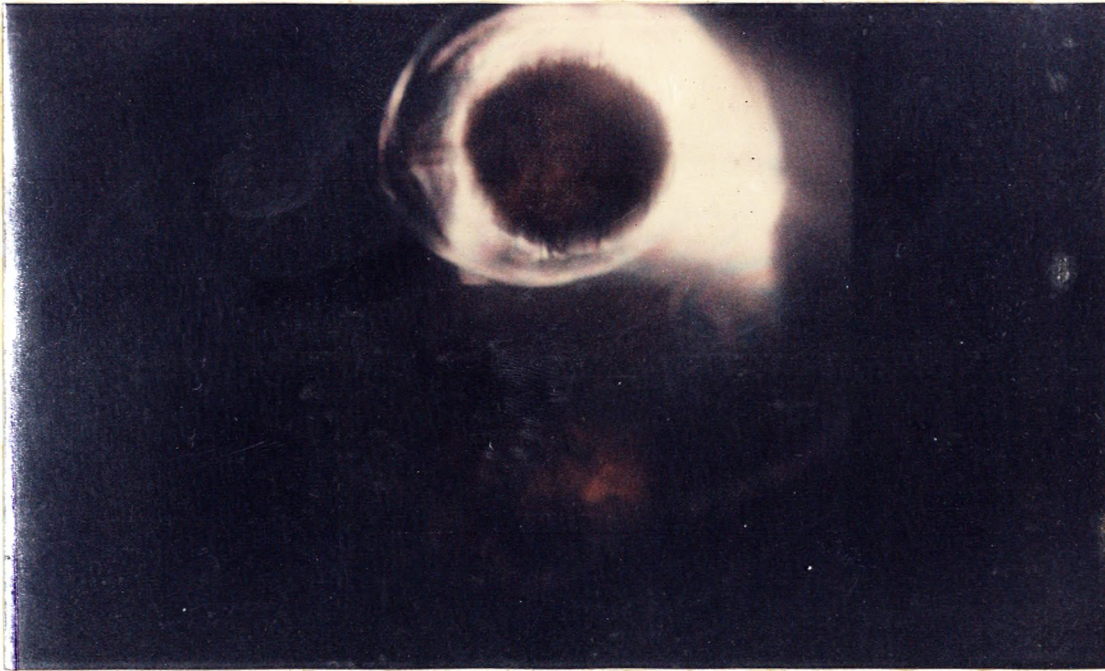


Figure E-11: Plexiglas Test No. 1: Continuous Plexiglas Model Test. 30.0 Microseconds after Firing

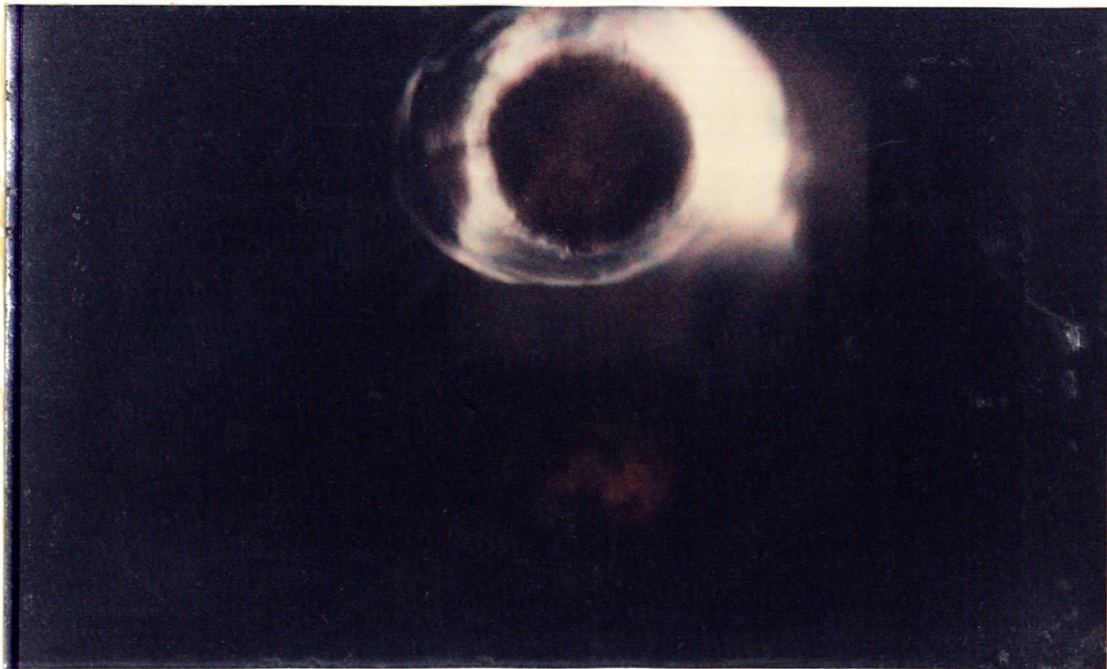


Figure E-12: Plexiglas Test No. 1: Continuous Plexiglas Model Test. 32.5 Microseconds after Firing

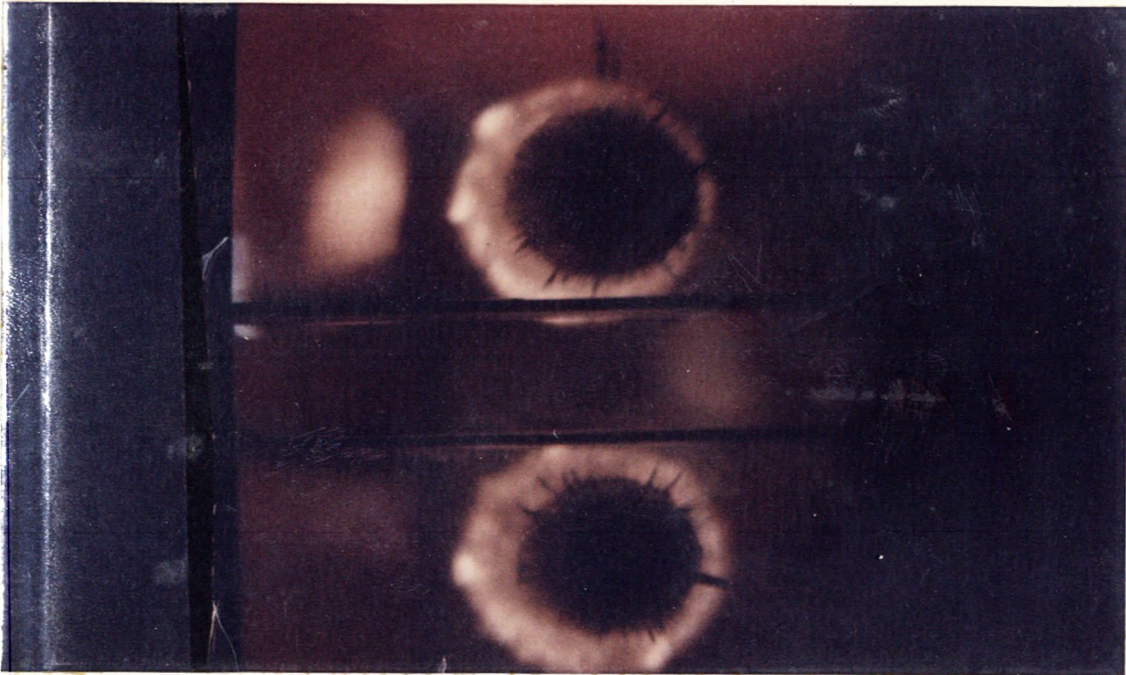


Figure E-13: Plexiglas Test No. 2: 1/16 in.
Sand Filled Two-Joint Model Test

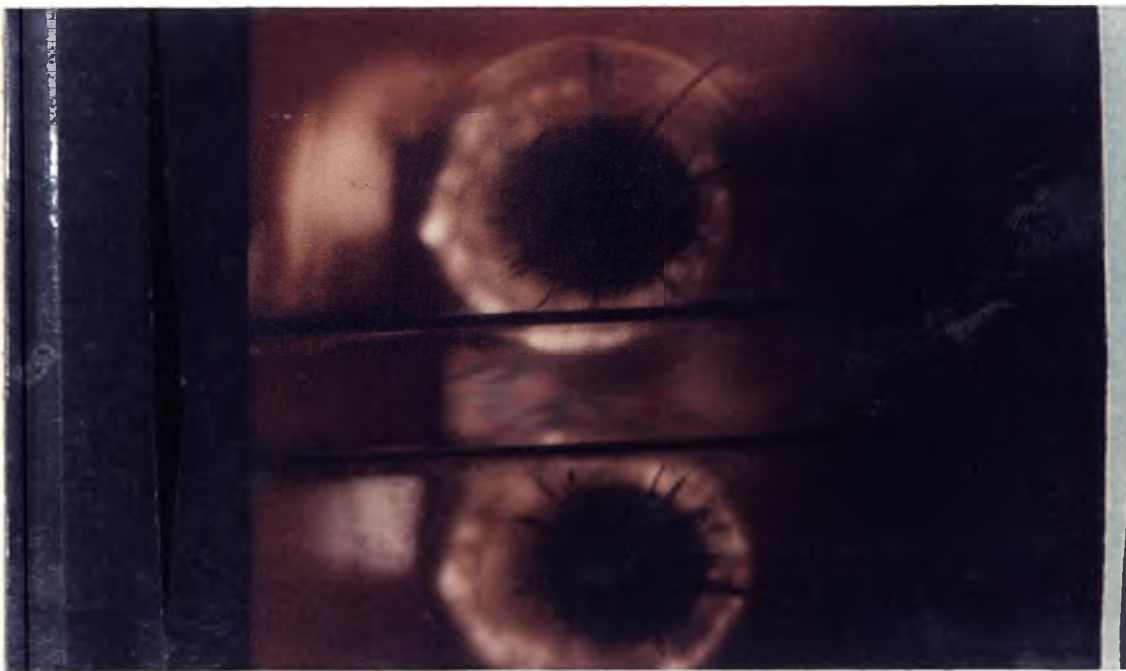


Figure E-14: Plexiglas Test No. 2: 1/16 in.
Sand Filled Two-Joint Model Test,
Photographed after Figure E-13

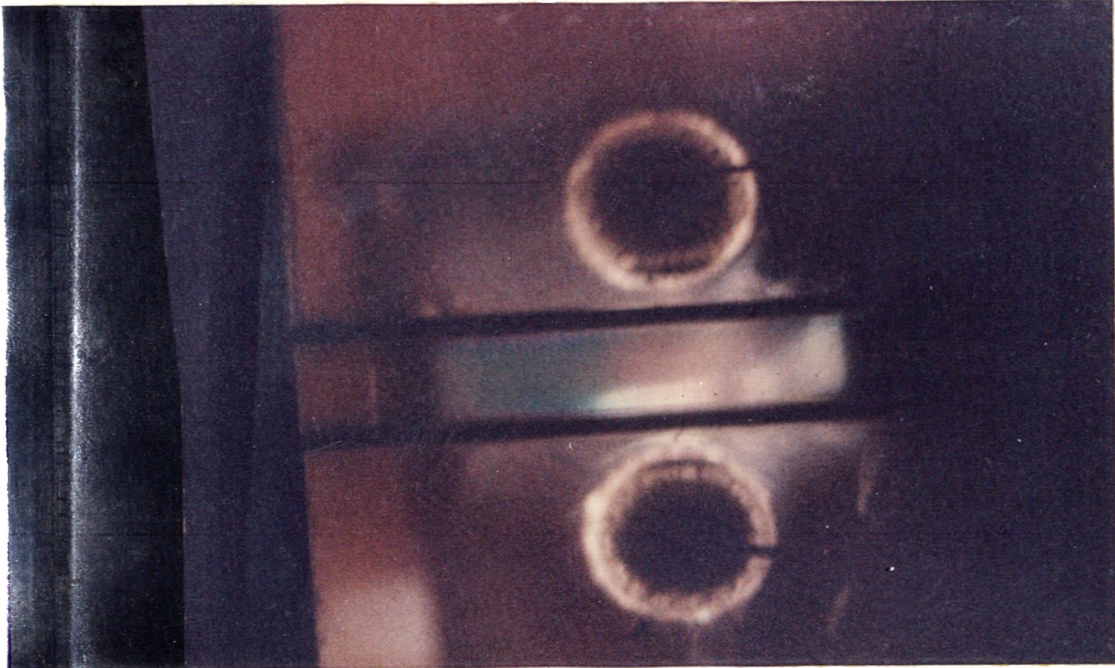


Figure E-15: Plexiglas Test No. 3: 1/8 in.
Sand Filled Two-Joint Model Test

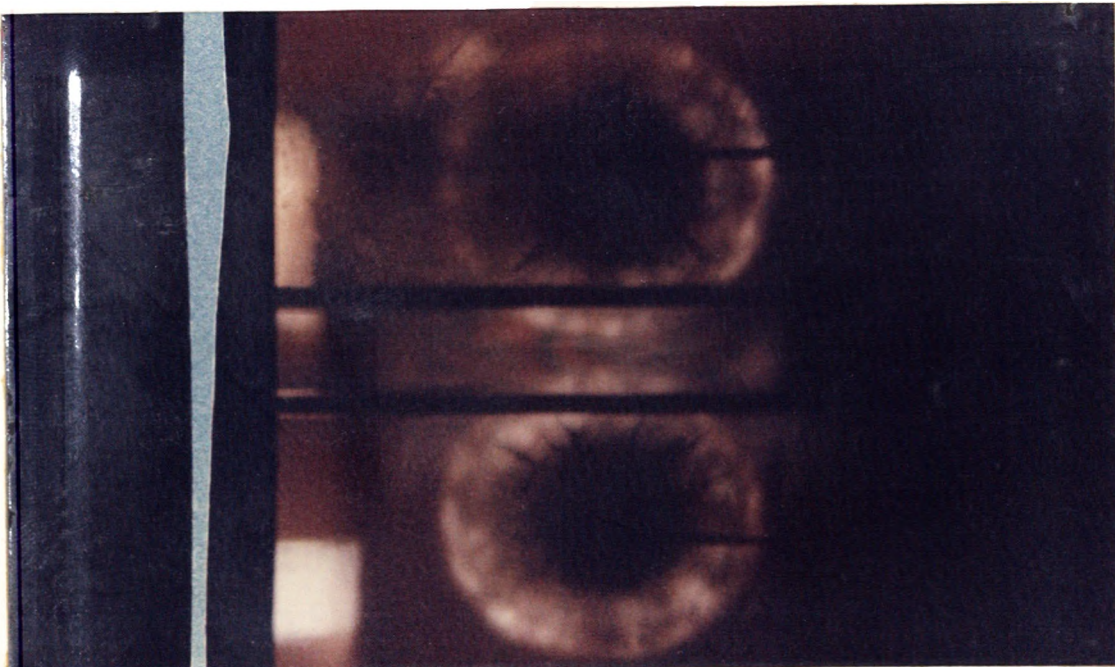


Figure E-16: Plexiglas Test No. 3: 1/8 in.
Sand Filled Two-Joint Model Test,
Photographed after Figure E-15

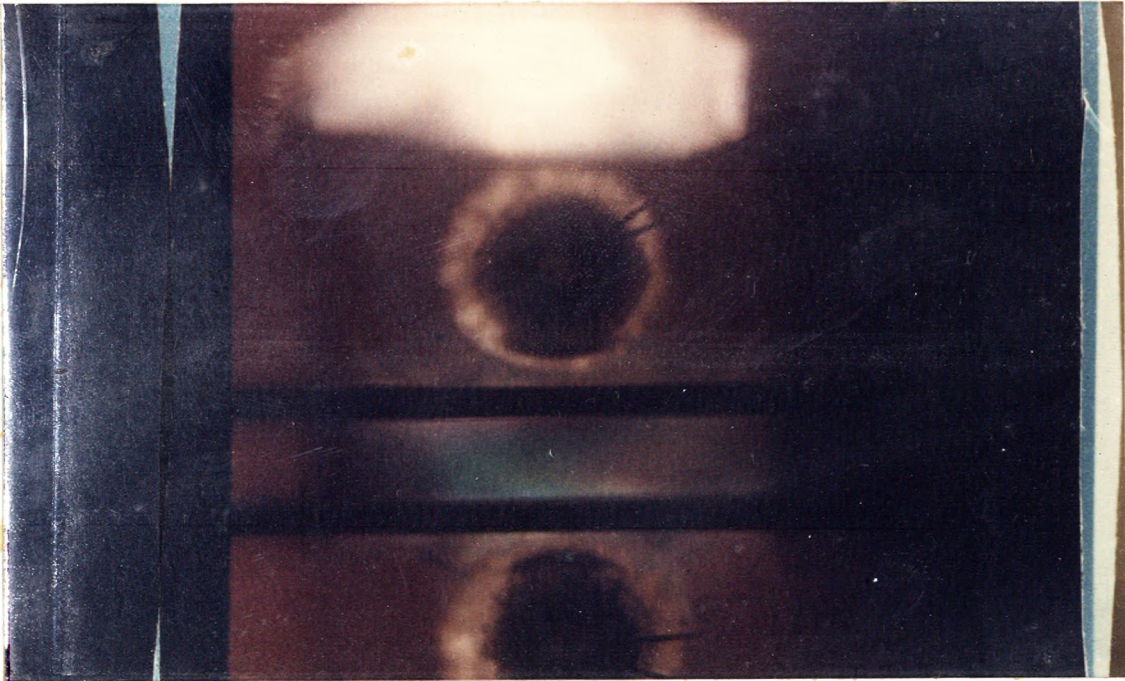


Figure E-17: Plexiglas Test No. 4: 1/4 in.
Sand Filled Two-Joint Model Test

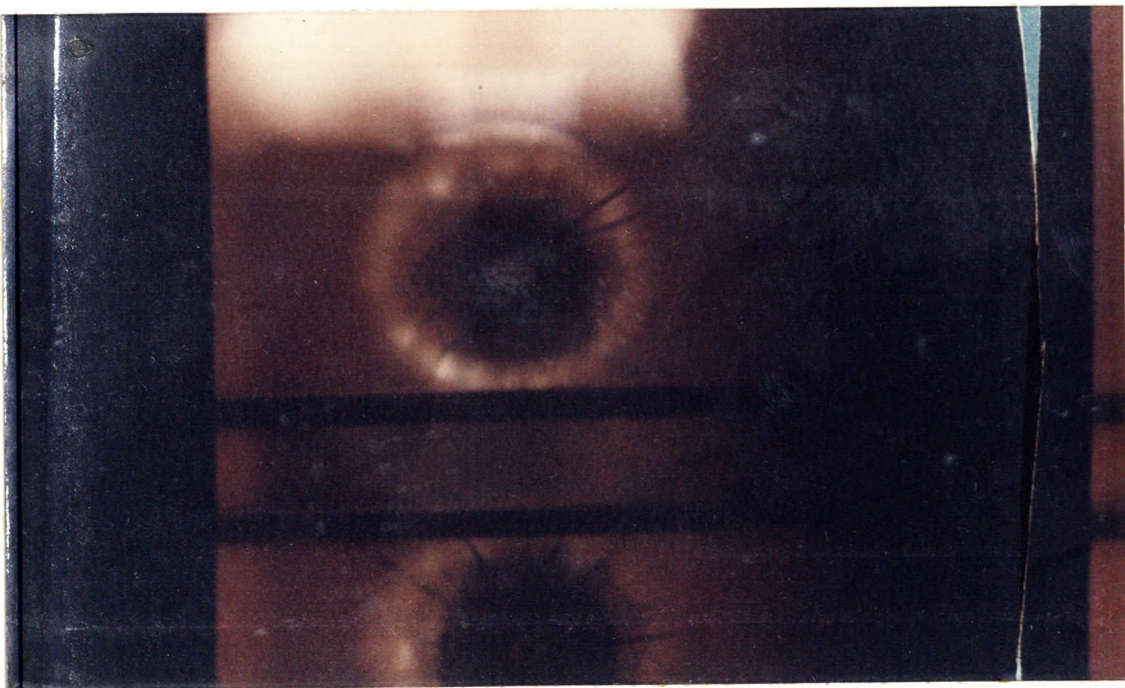


Figure E-18: Plexiglas Test No. 4: 1/4 in.
Sand Filled Two-Joint Model Test,
Photographed after Figure E-17

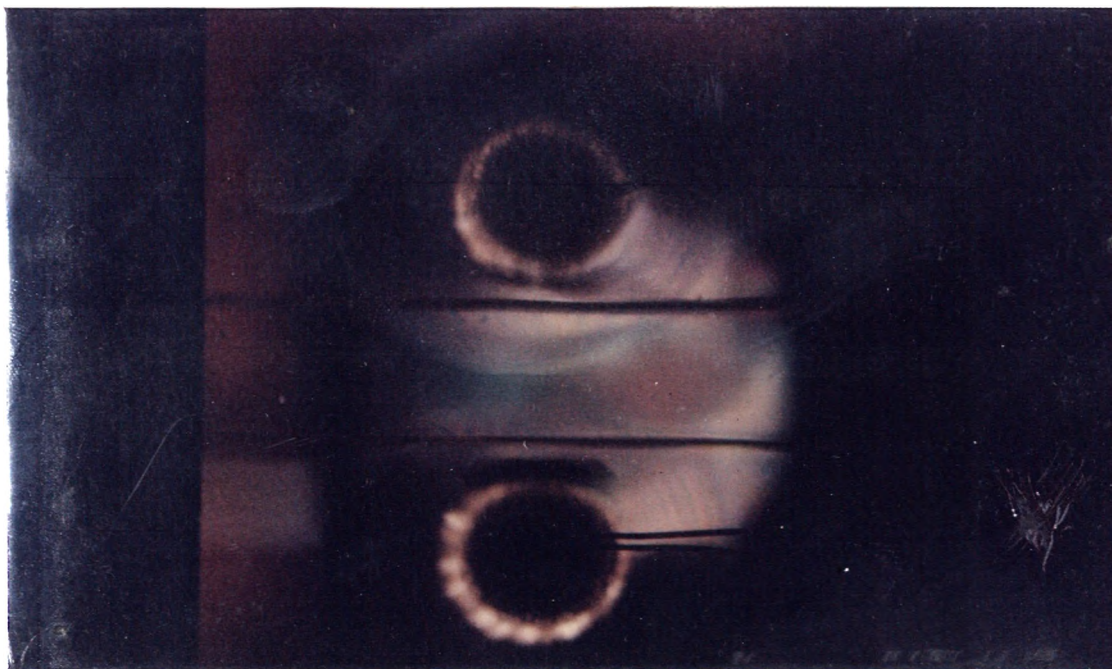


Figure E-19: Plexiglas Test No. 5: Two Closed
Joint Model Test

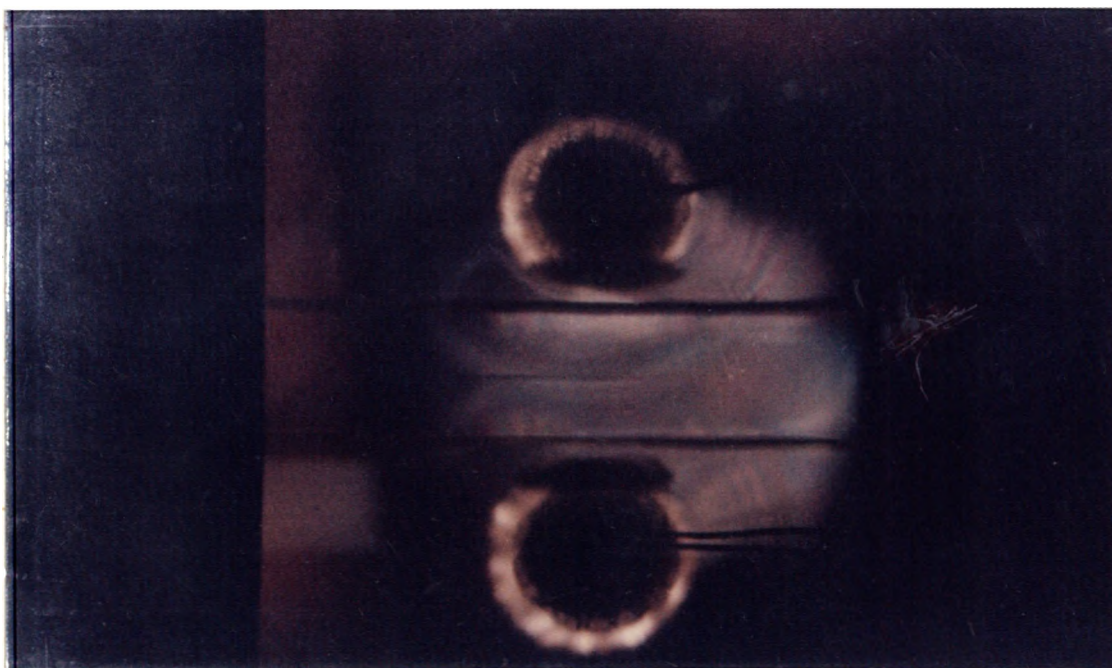


Figure E-20: Plexiglas Test No. 5: Two Closed
Joint Model Test, Photographed
after Figure E-19

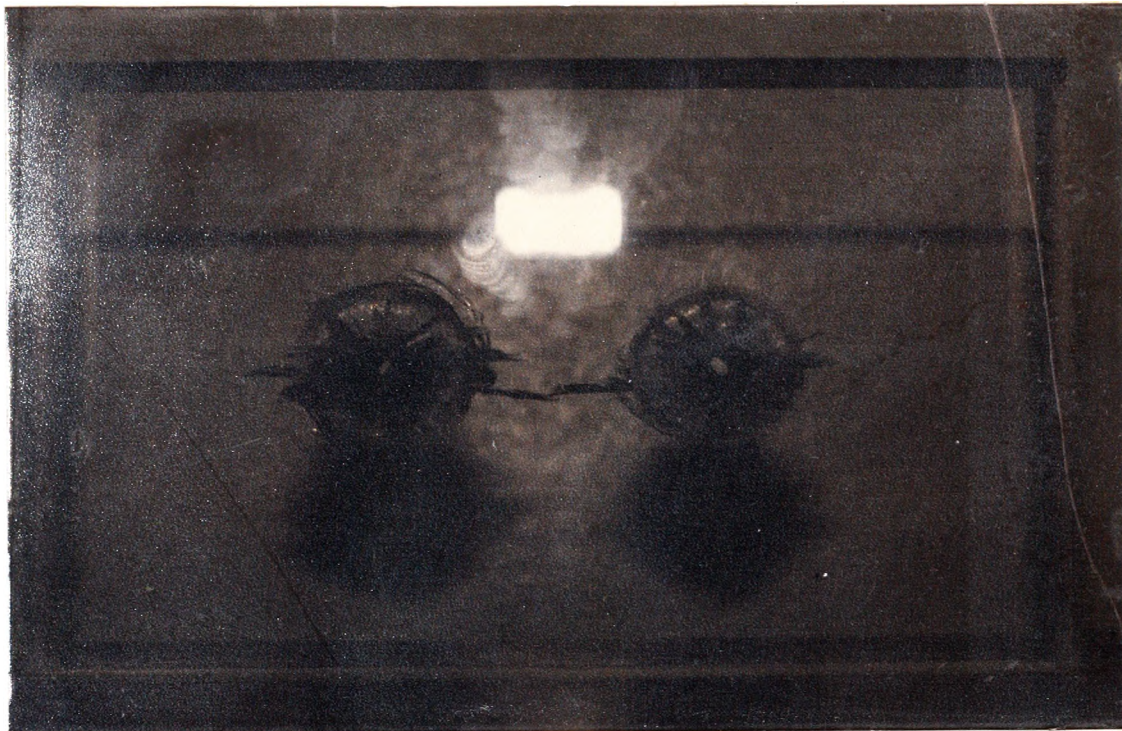


Figure E-21: Post-test Picture of Test No.1,
Showing the Pattern of Cracks in
the Continuous Plexiglas Test Model



Figure E-22: Post-test Picture of the Test No.4,
Showing the Cratering Effect in the 1/4 in.
Sand Filled Two-Joint Plexiglas Test